



Phosphorus transport in a hotter and drier climate: in-channel release of legacy phosphorus during summer low flow conditions

Christine L. Dolph¹, Jacques C. Finlay¹, Brent Dalzell^{2,3}, Gary W. Feyereisen^{2,3,4}

5 ¹Department of Ecology, Evolution and Behavior, University of Minnesota, 140 Gortner, 1479 Gortner Ave, St. Paul, Minnesota, 55108

²USDA-ARS Soil and Water Management Research Unit, St. Paul, Minnesota, 55108

³Department of Soil, Water, and Climate, University of Minnesota, 438 Borlaug Hall, 1991 Upper Buford Circle, St. Paul, Minnesota, 55108

10 ⁴Department of Bioproducts and Biosystems Engineering, University of Minnesota, 1390 Eckles Ave., St. Paul, Minnesota, 55108

Correspondence to: Christine L. Dolph (dolph008@umn.edu)

Abstract. The release of bioavailable phosphorus (P) during hot, dry summer periods when conditions are optimal for algal growth in lakes and rivers drives increased eutrophication risk. In addition to external P inputs, water quality is impacted by “legacy P”, i.e., the historical accumulation of P in soils and sediments due to past inputs. River networks represent a potential sink and/or source of legacy P, with many dynamic in-channel processes potentially governing the storage and mobilization of P over time. The objective of this study was to evaluate the potential contribution of in-channel release of legacy P to bioavailable P transport in streams during summer low flow conditions across a land use gradient in Minnesota, USA. We hypothesized that in-stream release of legacy P contributes to elevated concentrations of bioavailable P (i.e., soluble reactive P, SRP) during summer in streams with strong agricultural and/or urban influence, in addition to concurrent contributions from tile drainage systems and point source discharges. We addressed this hypothesis through synthesis of three water quality datasets: 1) water quality and stream flow (Q) data collected for 143 gaged watersheds across the state of Minnesota between 2007-2021 (22,750 total samples); 2) water quality data from 33 additional ditch, stream and river sites in Minnesota sampled under low flow conditions in summer of 2014; and 3) water quality data collected from tile drainage outlets for 10 monitored farm fields between 2011-2021. We used geospatial data and a machine learning (random forest) approach to identify possible drivers of bioavailable P concentrations during summer low flows for gaged watersheds. Our analysis indicates that between one third to one half of the gaged watersheds we studied exhibited SRP concentrations during low flows in late summer above previously identified thresholds for eutrophication of 0.02 - 0.04 mg/L. For many of these watersheds, stream SRP concentrations in late summer were above those observed in tile drainage outlets. Elevated SRP concentrations during late summer low flows weakened concentration-discharge relationships that would otherwise appear to indicate more strongly mobilizing SRP-Q responses across other seasons and flow conditions. We found that while wastewater discharge contributed to elevated P concentrations for watersheds with high densities of treatment plants, many did not have substantial wastewater impacts. The most important variables for predicting bioavailable P concentrations during late summer low flow conditions in a random forest model were land use in riparian areas (particularly crop cover), soil characteristics including soil erodibility, soil permeability, and soil clay content, agricultural intensity (reflected via higher pesticide use, higher phosphorus uptake by crops, and higher fertilizer application rates), as well as watershed precipitation and stream temperature. These findings suggest that, for stream and river sites heavily



40 impacted by past and current P inputs associated with agriculture and urbanization, biogeochemical processes mediated by climate and geology result in the release of legacy P from in-channel stores during late summer low flow conditions. As summers become hotter and, at times, drier -- predicted changes in this region -- conditions for the release of legacy P stored in stream and river channels will likely become more prolonged and/or more acute, increasing eutrophication risk.

45 **Short Summary**

“Legacy Phosphorus” is the accumulation of phosphorus (P) in soils and sediments due to past inputs from fertilizer, manure, urban runoff, and wastewater. The release of this P from where it is stored in the landscape can cause poor water quality. Here, we used examined whether legacy P is being released from stream and river channels in summer across a large number of watersheds, and we examined what factors (such as climate, land use and soil types) might be driving that release.

50



1 Introduction

55 Phosphorus (P) inputs arising from urbanization and industrial/intensive agriculture have resulted in widespread eutrophication of freshwater and marine environments. Excessive inputs of P along with nitrogen (N) have resulted in costly and sometimes dangerous conditions for human society, including increased prevalence of harmful algal blooms, contamination of drinking water supplies, decreased recreational opportunities, loss of critical marine fisheries, and negative impacts to biodiversity (Bennett et al., 2001). This problem is particularly acute in the Midwestern Cornbelt of the United States, which represents a global hotspot for P fertilization (Haque, 2021).

60 Most progress in reduction of P release to the environment has come from the implementation of improved wastewater infrastructure (Keiser and Shapiro, 2018). However diffuse (nonpoint) sources of P such as those arising from agricultural and urban landscapes have yet to be substantially curtailed and remain largely unregulated. In addition to ongoing P inputs to the environment, water quality is also impacted by the existing supply of “legacy P” in the landscape (Goyette et al., 2018). Legacy P is the historical accumulation of P in soils and sediments due to past land
65 use practices, such as agricultural fertilization, the spreading of manure, and wastewater discharge.

Efforts are underway to understand sources of legacy P in the terrestrial environment including agricultural soils and riparian buffers (e.g., Osterholz et al., 2020). Lentic water bodies (lakes, impoundments and wetlands) are well known for their potential to remobilize stored P and become sources instead of sinks for downstream P, especially at high rates of nutrient inputs (e.g., Vilmin et al., 2022). The river network itself represents another potential sink and/or
70 source of legacy P; with many dynamic in-channel processes potentially governing the storage and mobilization of P over time. For example, benthic redox conditions, in-stream primary productivity, microbial respiration, and sediment adsorption-desorption can all modulate whether P is retained in stream sediments, temporarily immobilized as organic P, or released to the water column as bioavailable P (Records et al., 2016).

We previously observed that concentrations of bioavailable P (i.e., soluble reactive phosphorus, SRP) in agriculturally-
75 dominated streams and rivers of Minnesota were often elevated during low flow conditions in late summer (Dolph et al., 2019). However, questions remained about whether the elevated SRP we observed in late summer was sourced predominantly from tile drainage (i.e., and therefore indicative of legacy and/or current P sources stored in farm soils), from point sources such as wastewater treatment plants, or possibly from legacy sources in the river network itself. Tile drainage is extensive across the agricultural Midwest (Valayamkunnath et al., 2020) and has been found to
80 contribute substantially to and even dominate soluble P export in agricultural watersheds (King et al., 2014; Smith et al., 2015). P concentrations in tile waters have been found to be highest during summer compared to other seasons (King et al., 2014), and therefore represent a possible driver of elevated SRP in streams and rivers receiving tile drainage at this time of year. Comparatively high SRP concentrations during low flows can also be indicative of the dominance of point discharges; these concentrations are often diluted under wetter conditions (Dupas et al., 2023).
85 Alternatively, however, there is some indication that groundwater and/or in-channel processes may drive the release of bioavailable P in river channels at some times of year (Schilling et al., 2020; Vissers et al., 2023).



A number of recent papers have examined potential legacy P dynamics in streams and rivers; these studies have typically been deployed at the reach scale (i.e., stream reaches of a few hundred meters or less), or for individual small to medium-sized watersheds (e.g., Bieroza and Heathwaite, 2015; Casquin et al., 2020; Kreling et al., 2023; Siebers et al., 2023; Vissers et al., 2023; Dupas et al., 2023; Rode et al., 2023). These in-depth studies are important and highly useful, as the microscale dynamics governing P mobility in river channels can be complex. However, few studies have examined the potential contribution of in-channel legacy P at larger regional scales, or across a large number of watersheds.

90

95

100

The objective of this analysis was to determine the potential contribution of in-channel legacy P sources to SRP transport under summer low flow conditions across a relatively broad spatial scale (i.e., the state of Minnesota). We hypothesized that in-stream processes contribute to elevated concentrations of bioavailable P during summer in streams with strong agricultural and/or urban influence, in addition to the contribution of tile drainage systems and point source discharges. We addressed this hypothesis through synthesis of three water quality datasets: 1) water quality and stream flow data collected for 143 gaged watersheds across the state of Minnesota between 2007-2021 (22,750 total samples); 2) water quality data from 33 additional ditch, stream and river sites in Minnesota sampled under low flow condition in summer of 2014; and 3) water quality data collected from tile drainage outlets for 10 monitored farm fields between 2011-2021. We also used geospatial data and a machine learning approach to identify possible drivers of elevated SRP concentrations during summer low flows for gaged streams and rivers.

105

Watersheds across the state of Minnesota span a land use gradient from those dominated by intensive agriculture typical of the Upper Midwest region, to a major metropolitan area, to areas of heavy forest and wetland cover with comparatively fewer historic P inputs. This gradient provides a useful contrast that can potentially be applied to identify differential behavior of streams and rivers strongly impacted by legacy P.

2 Methods

2.1 Study area

110

The study area for this research spans the entire state of Minnesota, USA, encompassing approximately 225,163 km² within the Upper Midwestern region of the United States (Fig. 1). The state includes parts of four major drainage basins: the Upper Mississippi River Basin in the central, south and southeastern portions of the state, the Red River Basin in the northwest, the Great Lakes Basin in the northeast and the Upper Missouri River in the far southwest corner. Gradients in land use, soils, and precipitation vary from north to south and east to west (Fig. 1). The majority of the southern and north-western parts of the state are dominated by industrial row crop agriculture, predominantly corn and soybeans, with a high density of concentrated animal feeding operations (CAFOs) particularly in the south. By contrast, the north and northeastern parts of the state are dominated by forest and wetland cover. The state is also home to a major metropolitan area, encompassing the Twin Cities of Minneapolis and St. Paul and the surrounding seven counties (population of 3.69 million, 2020 US census) characterized by urban and suburban landscapes.

115

120

Precipitation varies from driest in the northwest (annual average rainfall ~550 mm, 1991-2020) to wettest in the southeast (annual average rainfall ~950 mm, 1991-2020; Johnson et al., 2022). Mean annual temperatures are higher in the south (annual average temperature ~ 7°C, 1991-2020) and lower in the north (annual average temperatures ~ 2-



3°C, 1991-2020). The entire state is characterized by a cold climate, with average winter temperatures well below freezing and with considerable snowfall historically expected most years. Most soils are formed from glacial and periglacial deposits. Soil textures range from sandy soils in the central part of the state, clay loam and silty clay loam soils in the south-central and southwest, and outwash till over karst bedrock in the southeast. Many of the soils in the western part of the state are calcareous with high pH. Water quality in the state is characterized by widespread impairments in the agriculturally and urban dominated regions, with the most ubiquitous impairments attributed to turbidity, total phosphorus, fecal coliform, impaired biota, and low dissolved oxygen (MPCA, 2022). Water quality in the northeastern part of the state is comparatively good, with lower levels of nutrient enrichment, although impairments for mercury contamination arising from coal burning and subsequent atmospheric deposition are widespread.

2.2 Overview of study data

For this study, we utilized three independent datasets (Fig. 1):

1) SRP concentration and discharge data (total n=22,750 flow-matched water chemistry samples) collected for 143 gaged stream and river watersheds monitored by the state of Minnesota's Watershed Pollutant Load Monitoring Network¹ between 2007-2021. These data were used to evaluate SRP transport behavior and understand drivers of late summer SRP.

2) SRP concentration and discharge data available for 10 tiled farm fields across the state, collected between 2011-2021 by the Discovery Farms Minnesota program². These data were used to estimate seasonal SRP concentrations for tile outlets as a point of comparison with riverine SRP concentrations.

3) SRP grab samples collected during low flow conditions in late summer of 2014 for an additional set of ditch, stream and river sites. (n=33; Dolph et al., 2017a³). These data were used to provide additional information about SRP concentrations in smaller order systems that were underrepresented among gaged watersheds.

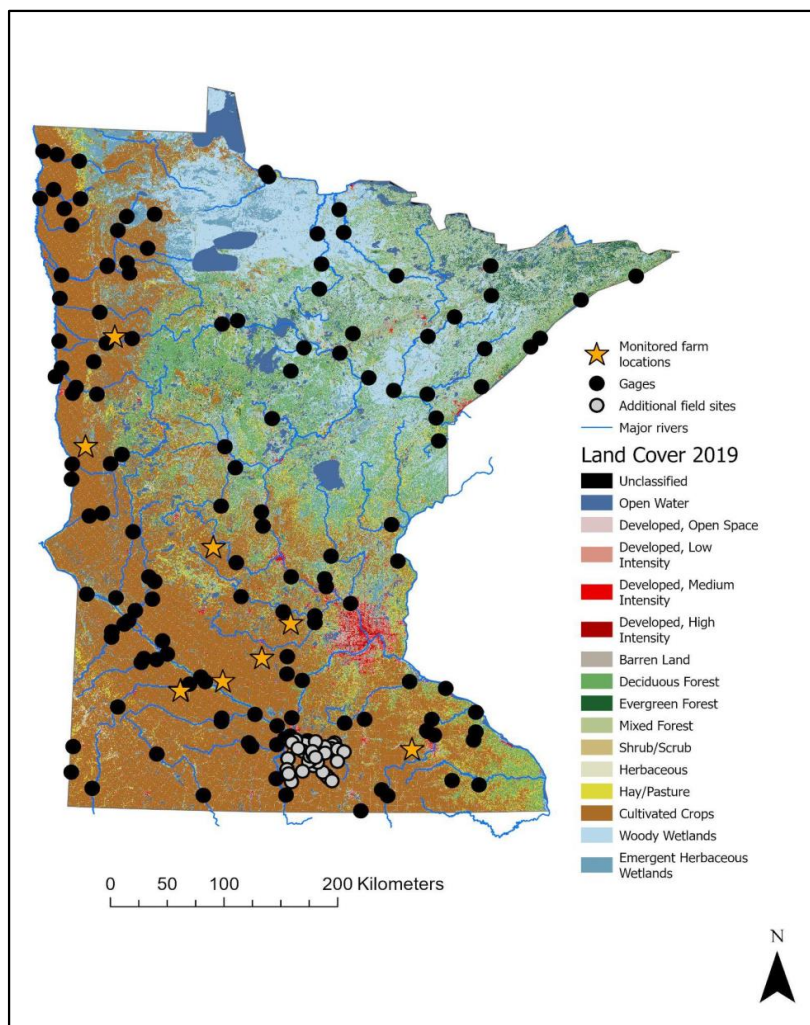
All data analysis was performed in R (R Core Team, 2023). Study data and R scripts used for data analysis are available at https://github.com/cldolph/instream_legacyP.

¹

<https://public.tableau.com/app/profile/mpca.data.services/viz/WatershedPollutantLoadMonitoringNetworkWPLMN/DataViewer/ProgramOverview>

² <https://discoveryfarmsmn.org/>

³ <https://conservancy.umn.edu/handle/11299/189907>



150 Figure 1: Locations of 1) 143 gaged stream and river watersheds intensively sampled for SRP and flow (total n=22,750
samples) at the watershed outlet during 2007-2021 (black dots; n=143). Data from these sites were used to evaluate SRP
transport behavior and understand drivers of late summer SRP; 2) Farm fields with tile outlet water quality available
155 (collected between 2011-2021; orange stars; n=10) used to estimate seasonal SRP concentrations for tile outlets, as a point
of comparison with riverine SRP concentrations; 3) ditch, stream and river sites sampled during summer low flow
conditions in 2014 (gray dots; n=33). Data from these sites were used to quantify late summer SRP concentrations in smaller
order systems.

2.3 Water quality data from stream and river gages

We used paired SRP and daily discharge data from 143 gaged stream and river watersheds (Fig. 1) monitored by
Minnesota's Watershed Pollutant Load Monitoring Network (WPLMN; note that the WPLMN also refers to SRP as
160 "dissolved orthophosphate"). The total number of samples across all gaged watersheds was 22,750. Periodic water
samples and continuous flow data were collected by the Minnesota Pollution Control Agency (MPCA) throughout the



165 year at major watershed sites (watershed areas greater than $\sim 4000 \text{ km}^2$) and during the period of ice-out through 31
October at smaller subwatershed sites (MPCA, 2015). Water quality sampling efforts were conducted \sim biweekly with
more intensive sampling focused on snowmelt and storm events, resulting in observations distributed across the range
of flows observed at each site (average # of samples per year = 25 for subwatersheds and 35 for major watersheds;
MPCA, 2015). The 143 gaged sites we selected for this study had >20 water chemistry samples collected across the
sampling period (2007–2021). Median number of water quality samples per site across the whole time period was 120
(min=21, max=478).

170 Watershed areas for gaged stream and river sites were assembled from multiple sources including existing watershed
delineations (n=11 watersheds) available from USGS (2012) and previously delineated watersheds (n=65 watersheds)
from Dolph et al., (2019), or delineated anew as part of the current study (n=68 watersheds). For newly delineated
watersheds, we used gage locations provided by Minnesota Department of Natural Resources and Minnesota Pollution
Control Agency (2023) as pourpoints, and existing flow direction and flow accumulation rasters available from the
NHDv2Plus dataset (USEPA, 2019) to delineate watersheds using the Spatial Analyst toolbox in ArcGIS Pro (ESRI,
175 2022). Watersheds were inspected visually and manually corrected for inaccuracies in delineation. Across all gaged
sites, watershed area ranged from 20 km^2 – $29,145 \text{ km}^2$ (mean = $1,996 \text{ km}^2$)

2.4 Farm tile outlets

180 We used SRP concentration and discharge data from tile outlets draining 10 farm fields across the state, measured
between 2011-2021 (Fig. 1). These tile outlets are monitored by the Discovery Farms Minnesota (DFM) program⁴.
The DFM is a farmer-led water quality research and educational program with the goal of collecting water quality
information under real-world conditions to support the development of better farm management decisions. During the
time of data collection, all monitored farm fields were planted in corn and soybean row crops grown in rotation. Two
sites (WR1 and ST1) included dairy operations, and two sites (BE1 and DO1) included swine finishing, in addition to
185 row crops.

The drainage areas for monitored farm fields ranged from 10-160 acres (mean = 97 acres). Farm field soil textures
ranged from poorly drained silty clay loam, to well drained loam. Three of the farms (MC1, RE1, and WR1) each had
one surface inlet to the tile drainage system. All other inlets were subsurface. Water quality and flow data collection
is described in detail by MDA (2021). Briefly, tile outlets were monitored continuously for flow (15 min interval) via
190 area velocity sensors installed in the tile drains that measured both stage and velocity. Water quality samples were
collected by ISCO 6712 automatic samplers on an equal-flow increment (EFI) composite basis, whenever tile outlets
were flowing. Water quality samples were composited every 125mL. Following a runoff event, water quality samples
were collected and promptly transported to a state contract lab and measured for dissolved orthophosphorus (i.e., SRP)
along with other water quality constituents. From continuous flow and composited sample SRP concentrations, we
195 calculated a daily flow-weighted SRP concentration (daily C) as follows: 1) multiply composite concentrations by

⁴ <https://discoveryfarmsmn.org/>



paired continuous flow measures to estimate continuous (15 min) loads; 2) sum composite sample loads into daily loads; 3) divide daily load by summed daily flow to compute a daily flow-weighted concentration in mg/L. Seasonal SRP concentrations were calculated by taking the mean of daily SRP concentrations for each tile outlet during each season (Early winter: Nov-Dec; Late winter: Jan-Mar; Spring: Apr-May; Early summer: Jun-Jul; Late summer: Aug-Sept; Fall: Oct).

200

2.5 Additional field sites

Among gaged stream and river watersheds, small order systems (especially first through third order ditches and streams) are under-represented relative to their prevalence across the landscape. To get a better understanding of SRP concentrations in smaller order systems, we also examined late summer low flow SRP concentrations collected from 33 agriculturally-dominated ditches, streams and mid-sized rivers in the Le Sueur River Basin, Minnesota (Fig. 1). Data for these sites is part of a larger publicly available field dataset⁵ for the region and described in detail by Dolph et al. (2019). Briefly, SRP concentrations were determined for grab water samples collected from 33 sites during low flow conditions in August of 2014. Flow conditions at the time of sampling were characterized by flow at the gaged outlet of the major HUC8-scale watershed in which samples were collected (i.e., the Le Sueur River Basin), based on daily discharge data available from MNDR⁶. Although flow at watershed outlets is not precisely representative of flow conditions further upstream in the basin, we have shown previously that discharge conditions across study sites scaled reasonably well with drainage area (Dolph et al., 2017b). We sampled on August 14, 17, 20, and 26 of 2014, during which flow conditions at the watershed outlet ranged between 19-25th percentile of all daily flows available for this watershed. Sites were categorized as ditches, perennial streams and rivers, or intermittent streams and rivers according to their designation in the NHDPlusv2 (USEPA, 2019).

205

210

215

2.6 Low flow conditions

Part of our aim in this study was to identify whether in-channel dynamics, such as instream release of legacy P, may affect stream and river SRP concentrations and transport behavior. Thus, we sought to identify low flow conditions where we assumed in-channel processes were likely to dominate P dynamics. We identified 'low flow' conditions as those falling within the lowest 25% of all daily discharge conditions measured for each watershed during the period of record for that gage. We defined seasons as follows: Early winter (Nov-Dec); Late winter (Jan-Mar); Spring (Apr-May); Early summer (Jun-Jul); Late summer: (Aug-Sept); Fall (Oct). We calculated mean SRP during low flow conditions for each gaged watershed in each season, for gages that had a minimum of three SRP samples collected during low flow conditions in that season. Note that not all gaged watersheds had three or more SRP samples collected during low flows in each season (Table A4); thus, the number of gaged watersheds with mean low flow SRP values available for analysis was different during each season (this parallels the availability of low flow conditions across seasons, with low flows being most common during late summer compared to other seasons).

220

225

⁵ <https://doi.org/10.13020/D6FH44>

⁶ <https://www.dnr.state.mn.us/waters/csg/index.html>



We hypothesized that low flow SRP concentrations could be substantially affected by one or all of the following: tile outlet concentrations, wastewater treatment plant discharges, or riverine legacy P stores. To help discern these influences, we compared low flow riverine SRP concentrations to tile outlet concentrations. In addition, we evaluated low flow riverine SRP concentrations for gaged watersheds relative to wastewater treatment plant density (sites/km²) in the watershed. Wastewater treatment plant density estimates were obtained from the US EPA StreamCat dataset (Hill et al., 2016; see additional details about StreamCat below), and were based on wastewater treatment plants listed in EPA's Facility Registry Services and National Pollutant Discharge Elimination System (NPDES)⁷. We also evaluated low flow riverine SRP concentrations relative to % cropland land use in gaged watersheds, to examine the assumption that agricultural land use and the associated past and current P inputs might drive the supply of riverine P. Cropland land use estimates were also obtained from StreamCat and were based on the 2019 National Land Cover Database (Dewitz, 2021).

2.7 Influence of late summer low flows on concentration-discharge relationships

We evaluated the relationship between SRP concentration (C) and discharge (Q) using the power law relationship in Eq. 1:

$$C=aQ^b \tag{1}$$

where the curve's coefficient (a) and exponent (b) are representative of the degree, direction, and rate at which SRP is transported as a function of stream flow. This equation can alternatively be expressed in log-log scale as Eq. 2:

$$\log(C) = b \log(Q) + \log(a) \tag{2}$$

where b is the slope of the linear log-log relation, and $\log(a)$ is the y -intercept. Normalizing Q by the geometric mean of discharge (Q_{GM}) shifts the center of mass of the log-transformed Q data to the y -intercept, allowing for comparison of rating curves among different watersheds (Warrick et al., 2015). We performed linear regression of log-transformed SRP concentrations on log-transformed normalized discharge using Eq. 3:

$$\log(C) = b \log(Q/Q_{GM}) + \log(a) \tag{3}$$

All regressions were performed in R (R Core Team, 2023). We evaluated the fit of the power law relationship for all gaged watersheds using the significance value p , slope b and R^2 of the linear regression.

The slope b of this relationship describes the per unit increase in concentration as discharge increases. Concentrating relationships ($b > 0$) imply higher flows are mobilizing more of a waterborne constituent, particularly through erosion or greater landscape connectivity. Diluting relationships ($b < 0$) suggest that constituents are source-limited or that relatively consistent inputs are diluted by greater discharge (Godsey et al., 2009). When b is near 0, C - Q relationships may be either chemostatic (i.e., relatively constant concentrations across the range of discharge conditions), or chemodynamic (i.e., concentrations are highly variable across the range of discharge conditions but not linearly related to flow). Chemostatic behavior has been observed for mineral weathering products or for constituents with large legacy

⁷ <https://catalog.data.gov/dataset/epa-facility-registry-service-frs-wastewater-treatment-plants>



260 sources like nitrate (Godsey et al., 2009; Basu et al., 2010; Musolff et al., 2015), whereas chemodynamic behavior may indicate that biogeochemical processes such as sorption/desorption, biotransformation or oxidation/reduction strongly affect nutrient transport behavior (e.g., Wanner et al., 1989). To distinguish between these two behaviors, we evaluated the coefficient of variation of C relative to the coefficient of variation of Q (CV_C/CV_Q). A $CV_C/CV_Q < 1$ suggests that concentrations are relatively constant compared to variability in flow, indicating chemostatic behavior. 265 By contrast, a larger CV_C/CV_Q indicates chemodynamic behavior (i.e., comparatively large variations in concentration relative to variation in flow). Thompson et al. (2011) suggested that CV_C/CV_Q values ≈ 0.3 could be used as a threshold to identify chemostatic vs chemodynamic behavior.

To determine the influence of low flow conditions in late summer on the nature of the C - Q relationships for all watersheds, we refit power law relationships to all watersheds after excluding SRP samples that were collected during 270 late summer low flow conditions. We compared regression parameters (p , slope b and R^2) before and after withholding samples collected during late summer low flow conditions, to determine if these samples had a widespread effect on C - Q relationships for SRP across gaged watersheds.

2.8 Regression analysis

2.8.1 Random Forest models

275 We used random forest modeling to identify possible predictors of SRP during low flow conditions in late summer for gaged stream and river watersheds. Random forest regression is a nonparametric ensemble learning method that utilizes predictions from multiple decision trees to improve model accuracy. Each tree is composed of branches (“nodes”) representing yes–no questions where features (i.e., predictive variables) are used to split the dependent variable into two groups that minimize in-group variability and maximize between group variability. We selected a 280 random forest approach because these models require few assumptions about data structure (i.e., data need not conform to assumptions of classical statistics such as linearity, normality, and constant variance), are robust to outliers, and generally perform as well or better than other data intensive approaches (Hagenauer et al., 2019). The use of random forest models also allows for the identification of predictors that are important to model accuracy, using measures such as condition permutation importance and post-hoc partial dependence plots (see additional details below).

285 2.8.2 Predictor Variables

Predictor variables for random forest (RF) models were assembled from the U.S. EPA StreamCat dataset⁸. StreamCat contains information for over 600 different environmental metrics linked to individual stream reaches in the NHDv2Plus dataset (Hill et al., 2016). These metrics summarize diverse geospatial attributes—including aspects of land cover, impervious surfaces and road density, soil type, point source and nutrient inputs, and climatic factors 290 (temperature and precipitation), among others—at the catchment and watershed scale draining into each reach. “Catchments” (i.e., local drainage areas) include the immediate land area draining into each individual stream reach in the NHD excluding areas draining to upstream reaches; “watersheds” include the entire land area draining into each stream reach. StreamCat contains land use data for catchments and watersheds summarized from the National Land

⁸ <https://www.epa.gov/national-aquatic-resource-surveys/streamcat-dataset>



295 Cover Database (NLCD) for multiple years. We used land cover attributes only from the 2019 iteration of the NLCD
for each gaged watershed using estimates of tile density (i.e., area tiled per area watershed)
for each gaged watershed using estimates of tiled areas (30 m resolution) from Valayamkunnath et al. (2020). Prior to
developing a random forest model, we excluded predictors from the StreamCat dataset that did not contain useful
information (i.e., all rows=0). We also excluded attributes where information was missing ('NA') for >20% sites.
Some of the remaining attributes still contained some missing values. Because random forest models cannot handle
300 missing values in predictor variables, we used the *missRanger* package in R (Mayer, 2023) to impute the remaining
missing values for the training and testing datasets. Prior to random forest modeling, we normalized (i.e., centered and
scaled) numeric attributes to have a mean of zero and a standard deviation of one.

2.8.3 Model Tuning and Selection

305 We developed the random forest model to predict mean SRP during late summer low conditions, based on data for
127 gaged watersheds. Only 128 of the 143 total gaged watersheds in the study had ≥ 3 SRP samples collected during
late summer low flow conditions and were therefore used to calculate mean SRP values. Prior to model development,
we excluded one additional site from the testing dataset (Buffalo Creek near Glencoe, MN) that had a mean SRP value
for late summer that exceeded the range of SRP values in the training dataset (see Appendix Fig. S1). To develop the
RF model, we used the same general approach to random forest modeling described in detail by Dolph et al. (2023).
310 Data were split randomly into independent model training (70%, $n=88$) and model testing (30%, $n=39$) datasets. Using
the training dataset and the *ranger* package in R (Wright and Ziegler, 2017), we applied tenfold cross validation to
tune model hyperparameters across a range of possible values. K-fold cross validation can assist in avoiding model
over-fitting and works by partitioning training data into K equal sized “folds” (in our case 10). The model is iteratively
trained on various combinations of tuning hyperparameters across K-1 folds, leaving the remaining fold to evaluate
315 model performance for each combination. The hyperparameters selected for tuning were: *mtry* (i.e., number of
variables randomly sampled as candidates at each split) and *min_n* (i.e., the minimum number of data points in a
node). The *trees* hyperparameter (i.e., number of trees) was set to 1000 across all models. We defined a grid of 20
potential combinations of hyper-parameters using the *tune_grid()* function from the *tidymodels* collection of packages
in R (Kuhn et al., 2020). This approach draws hyperparameter values semi-randomly from parameter space such that
320 the various combinations cover the whole space of potential values. We selected hyperparameter values using out-of-
bag (OOB) RMSE and R^2 for the associated models. Once hyperparameter values were tuned, we reran the random
forest model using the *randomForest* package (Liaw and Weiner, 2002), to create a *randomForest* object that was
compatible with our selected measure of predictive variable importance (conditional permutation importance, see next
paragraph). We evaluated overall model performance using R^2 and RMSE between predicted and observed SRP values
325 in the independent test dataset (comprising 30% of the original dataset).

2.8.4 Variable importance

We used Conditional Permutation Importance (CPI) to evaluate the importance of predictors to model performance.
CPI aims to capture the dependence between a predictor and the response variable, conditionally on the values of all
other predictors. CPI can be used to assess how much each variable contributes to accurately predicting the response



330 variable, given what we know from all other predictive variables. We implemented the CPI approach from the
331 *permimp* package in R (Debeer and Stobl, 2021). In *permimp*, a threshold value, equal to $1 - p$ -value for the
332 association between predictor variables, is used to determine whether to include a predictor in the conditioning for the
333 predictor of interest. We used the default value for the threshold parameter in *permimp* (0.95; Debeer and Stobl,
334 2021).

335 While the CPI method can rank predictors in terms of their importance to model accuracy, it does not convey
336 information about the nature of the relationship between predictor variables and late summer SRP concentrations. To
337 visualize these relationships, we created partial dependence plots (PDPs) using the *partialPlot* function in R (part of
338 the *randomForest* package, Liaw and Weiner, 2002). These plots illustrate the change in predicted SRP concentration
339 when the values of one predictor are changed while all other predictors are kept constant at their original values
340 (Greenwell, 2017). We generated PDPs for the top 15 predictor variables identified as most important by the measure
341 of CPI.

3 Results

3.1 SRP concentrations at gaged watersheds during low flow

342 Across gaged watersheds, we expected SRP concentrations at low flow conditions to differ depending on the extent
343 of historic and current P inputs associated with anthropogenic land use. Most gaged watersheds in our study region
344 (90%, $n=128$) were substantially impacted by either agricultural or urban land use (defined here as watersheds with
345 $\geq 50\%$ crop cover and/or $\geq 10\%$ high intensity urban land use). The remaining watersheds ($n=15$) were characterized
346 as 'less impacted'.

347 Among watersheds with substantial agricultural or urban influences, mean low flow SRP concentrations were highest
348 in late winter, lowest in spring, and then increased progressively through early summer, late summer, fall and early
349 winter (Table 1).

350 However, there was large variation (3–4 orders of magnitude) in low flow SRP concentrations across sites in any
351 given season (range across all samples = 0.001–3.9 mg/L). For less impacted sites, seasonal low flow SRP
352 concentrations were also highest on average during late winter, although the absolute concentrations were much lower
353 than more heavily impacted sites. By contrast to more heavily impacted sites, mean low flow SRP concentrations at
354 less impacted sites dropped in spring and stayed steady through summer, and dropped slightly again in fall. Less
355 impacted sites showed comparatively low SRP concentrations and lower variability in low flow SRP concentrations
356 across sites or seasons (range 0.001–0.046 mg/L).



360 **Table 1: Mean, minimum and maximum low flow SRP concentrations (mg/L) for more heavily impacted gaged watersheds (>=50% crop cover and/or >=10% high intensity urban land use) and less impacted gaged watersheds<50% crop cover and < 10% high intensity urban land use), across seasons.**

Degree of anthropogenic disturbance	Season	Mean SRP	Min SRP	Max SRP
More impacted	Late Winter	0.1288	0.002	3.550
	Spring	0.0302	0.001	0.0384
	Early Summer	0.0387	0.001	0.526
	Late Summer	0.0549	0.001	1.350
	Fall	0.0691	0.002	1.595
Less Impacted	Early Winter	0.1171	0.002	3.900
	Late Winter	0.0084	0.0020	0.019
	Spring	0.0075	0.0020	0.031
	Early Summer	0.0057	0.0005	0.028
	Late Summer	0.0054	0.0005	0.046
	Fall	0.0037	0.0015	0.008
	Early Winter	0.0076	0.0015	0.030

3.2 Influences of wastewater treatment facilities (point sources) on riverine SRP concentrations at low flow

365 Mean SRP concentrations at low flow for gaged watersheds were significantly related to the density of wastewater treatment plants in the watershed during early winter, late winter, late summer, and fall but not in spring or early summer (Fig. 2). Part of the discrepancy across seasons may have been caused by the fact that few watersheds with a high density of wastewater treatment plants were sampled during low flows in spring and early summer. The relationship between mean low flow SRP and wastewater treatment plant density was strongest in early winter (though still somewhat weak overall; $R^2=0.26$) and comparatively weaker in other seasons (Appendix Table A1). These relationships were largely driven by watersheds where density of wastewater treatment plants was comparatively high (>0.005 sites/km²). When watersheds with wastewater treatment plant density > 0.005 sites/km² were excluded, we observed a persevering very weak significant positive relationship between wastewater treatment plant density and mean lowflow SRP during late summer and late winter ($R^2=0.04$ and 0.10, respectively), but not during any other season. (see Appendix Table A1).

370

375

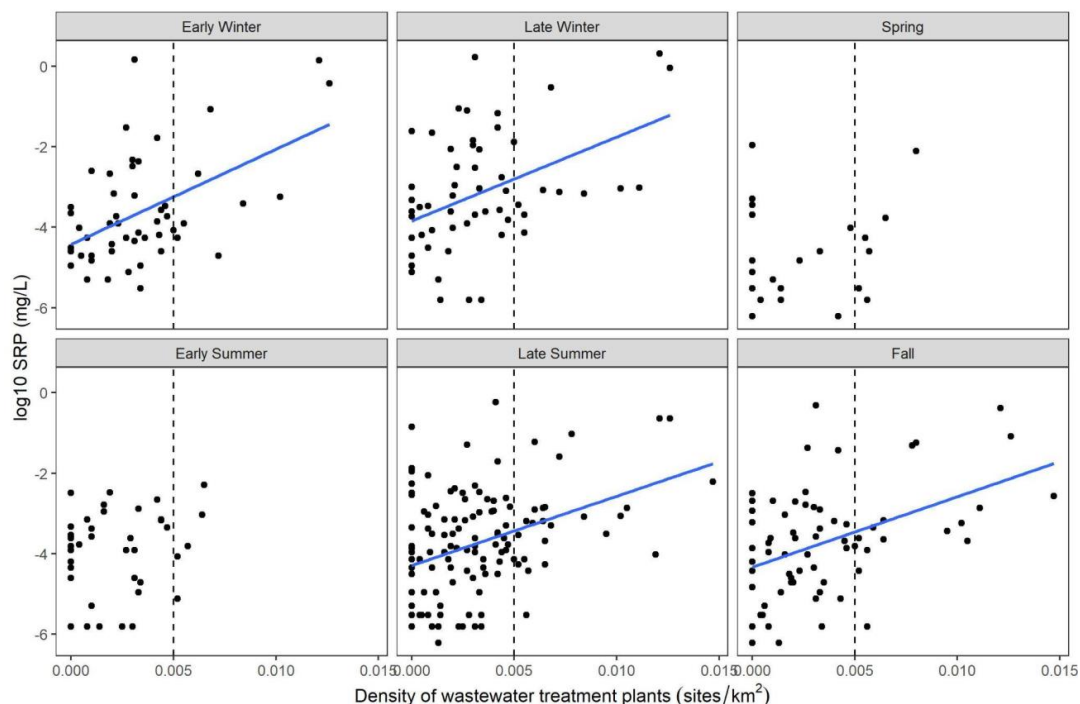


Figure 2: Relationship of SRP concentrations at low flows (log scale) in gaged watersheds to the density of wastewater treatment plants (sites/km²) in the watershed, by season. Blue lines indicate statistically significant linear regressions ($p < 0.05$). Linear regression statistics are shown in Appendix Table A1. Dashed line indicates wastewater treatment plant density of 0.005 sites/km². Note that not all gaged watersheds had sufficient samples collected during low flows in each season to generate mean values; thus, the number of gaged watersheds with low flow mean SRP values available was different during each season.

380

3.3 Riverine SRP at low flows in relation to agricultural land use

385

We observed consistent and positive relationships between agricultural land use (% cropland) and mean low flow SRP concentrations across gaged watersheds during all seasons, with the strongest relationships occurring during late summer and late winter (Fig. 3; Appendix Table A2). When we examined only sites without wastewater treatment plant influence, these relationships appeared even stronger, as evidenced by increased R^2 values (Fig. 4; Appendix Table A2). The strongest correlations were evident in late summer and late winter (R^2 of 0.69 and 0.86, respectively;

390

Fig. 4).

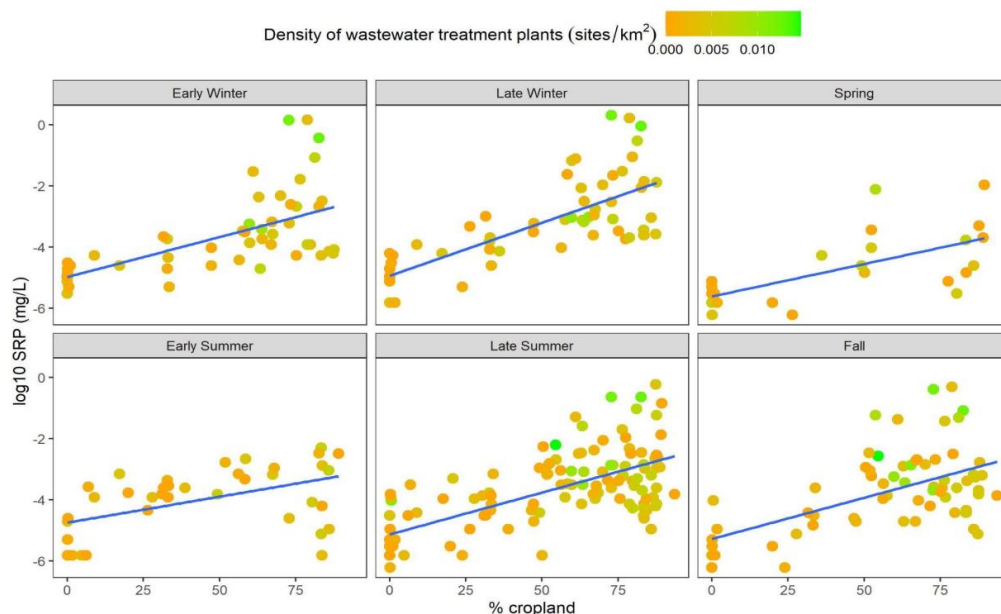


Figure 3: Mean low flow SRP concentrations across gages (log scale), in relation to % crop cover, by season. Color scale indicates density of wastewater treatment plants in the watershed. Relationships in all seasons were significant and positive. Linear regression statistics are shown in Appendix Table A2.

395

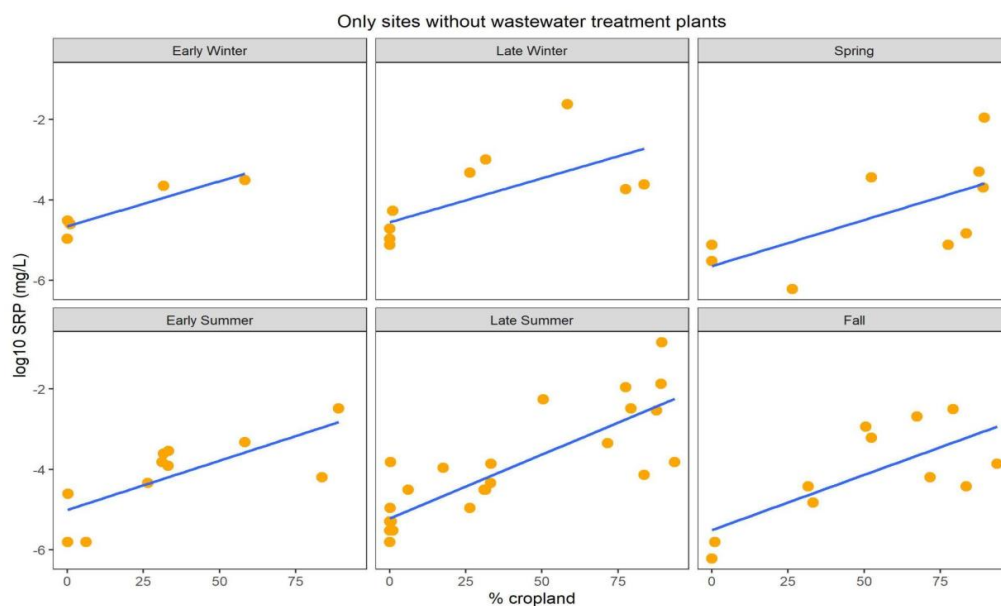


Figure 4: Mean low flow SRP concentrations across gages (log scale), in relation to % crop cover, by season, for sites with no wastewater treatment plant influence. Relationships in all seasons were significant and positive. Linear regression statistics are shown in Appendix Table A2.

400



3.4 SRP concentrations at tile outlets

Across tile outlets for 10 conventionally farmed fields (corn-soybean rotation), mean SRP concentration of tile drainage was highest in late winter (mean SRP = 0.12 mg/L) and lowest in early, late summer and early winter (mean SRP = 0.03 mg/L; Table 2). Two sites (WR1 and ST1) included dairy operations, and two sites (BE1 and DO1) included swine finishing, in addition to row crops. The two dairy-influenced farm fields (WR1 and ST1) had notably higher tile SRP concentrations across all seasons relative to other sites. Three sites (MC1 RE1, and WR1) had one surface inlet to the tile system (all other inlets were subsurface). These sites appeared to have higher mean SRP concentrations in late winter (coinciding with snowmelt) and early summer (in the case of MC1), but of the surface inlet sites only WR1 (the dairy farm site) had higher mean SRP concentrations in late summer.

Table 2: Mean flow-weighted daily SRP concentrations (mg/L) from farm tile outlets, by season. Tile outlet data were collected from farm sites between 2011-2021. Early winter: Nov-Dec; Late winter: Jan-Mar; Spring: Apr-May; Early summer: Jun-Jul; Late summer: Aug-Sept; Fall: Oct. ^aFarms included dairy operations. ^bFarms included a surface inlet to tile drainage system. ^cFarms included swine finishing.

Site	Early Winter	Late Winter	Spring	Early Summer	Late Summer	Fall	Annual mean
BE1 ^c	0.064	0.053	0.031	0.017	0.023	0.132	0.036
DO1 ^c	0.012	0.029	0.036	0.015	0.018	0.010	0.023
MC1 ^b	0.019	0.139	0.023	0.012	0.022	0.024	0.037
NO1W-N	0.008	0.011	0.018	0.015	0.016	0.008	0.014
NO1W-S	0.017	0.025	0.024	0.012	0.018	0.015	0.018
RE1 ^b	0.014	0.070	0.045	0.075	0.022	0.043	0.049
RW1N	0.023	0.231	0.025	0.014	0.011	0.033	0.061
RW1S	0.011	0.278	0.059	0.019	0.017	0.045	0.069
ST1 ^a	0.053	0.164	0.091	0.062	0.073	0.048	0.084
WI1	0.011	0.008	0.009	0.008	0.005	0.010	0.008
WR1 ^{a,b}	0.055	0.307	0.156	0.119	0.157	0.105	0.151
All sites	0.029	0.131	0.051	0.036	0.033	0.035	0.052



415 3.5 Riverine SRP at low flows compared to tile concentrations

We evaluated SRP during low flow conditions for each gaged watershed in each season (Table A3), and compared these riverine SRP values to SRP concentrations in monitored tile outlets. Note that not all gaged watersheds had sufficient samples collected during low flows in each season to generate mean values (Table A4); thus, the number of gaged watersheds with low flow mean SRP values available was different during each season. Comparisons for late winter, spring and late summer are shown in Fig. 5 (only a subset of seasons are shown for improved clarity in data visualization; similar figures for early winter, early summer and fall are shown in Appendix Fig. A2).

In early winter, 36% of gaged watersheds (n=18/50 sites for which low flow data was available) exhibited SRP concentrations at low flows that were higher than mean tile SRP concentration. Six of these watersheds were characterized by comparatively high wastewater treatment plant density (defined as >0.005 sites/km²). In late winter when tile SRP concentrations were highest, 23% of gaged watersheds (n=13/57) exhibited SRP concentrations at low flows that were higher than mean tile concentrations. Nearly all of these sites (12/13) had considerable wastewater treatment plant influence (wastewater treatment plant density > 0.005 sites/km²). In spring, SRP concentrations during low flow conditions were uniformly low across nearly all gaged watersheds. SRP samples collected during low flow conditions were fairly uncommon, with only 23 watersheds having ≥ 3 SRP samples collected during spring low flows. Of these, two sites (9%) had SRP concentrations at low flows that were higher than mean tile concentrations. In early summer (Jun-Jul), 28% of sites (n=11/40) had SRP concentrations at low flow that were higher than mean tile concentrations. Two of these sites had considerable wastewater treatment influence. In late summer (Aug-Sep), 39% of gaged watersheds (n=50/128) had SRP concentrations at low flow that were higher than mean tile concentrations, and 16 of these sites had considerable wastewater treatment influence. In fall (Oct), 35% of gaged watersheds (n=24/68) sites had SRP concentrations at low flow that were higher than mean tile concentrations; eight of these sites had comparatively higher wastewater treatment plant density.

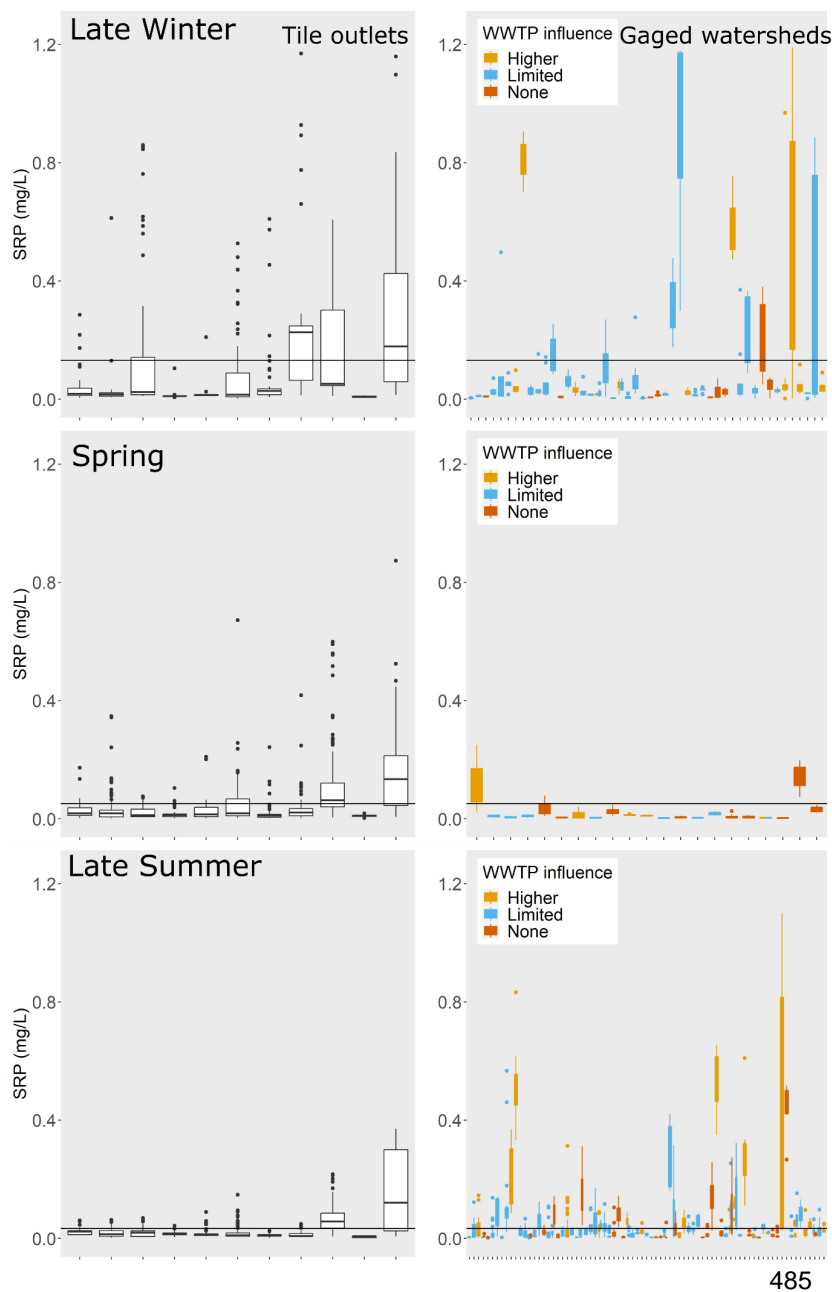


Figure 5: SRP concentrations (mg/L) for tile outlets and during low flow conditions for gaged watersheds, by season. Only a subset of seasons are shown for improved clarity in data visualization; similar figures for remaining seasons are shown in Appendix Fig. A2. The horizontal line in each plot is the mean SRP concentration among tile outlets for that season. For gaged watersheds, color of boxplots indicates degree of influence from wastewater treatment plants: light orange: wastewater treatment plant density >0.005 sites/km²; blue = wastewater treatment plant density <0.005 sites/km² but greater than zero; dark orange: no wastewater treatment plant sites in watershed. To improve data visibility, the y-axis for SRP was limited to a maximum of 1.25 mg/L, which eliminated a small number of outliers from the plots for tile outlets (n=34 out of 11,079 records) and gaged watersheds (n=16 out of 2,696 low flow records). Note that not all watersheds had sufficient samples collected during low flows in each season to generate boxplots.

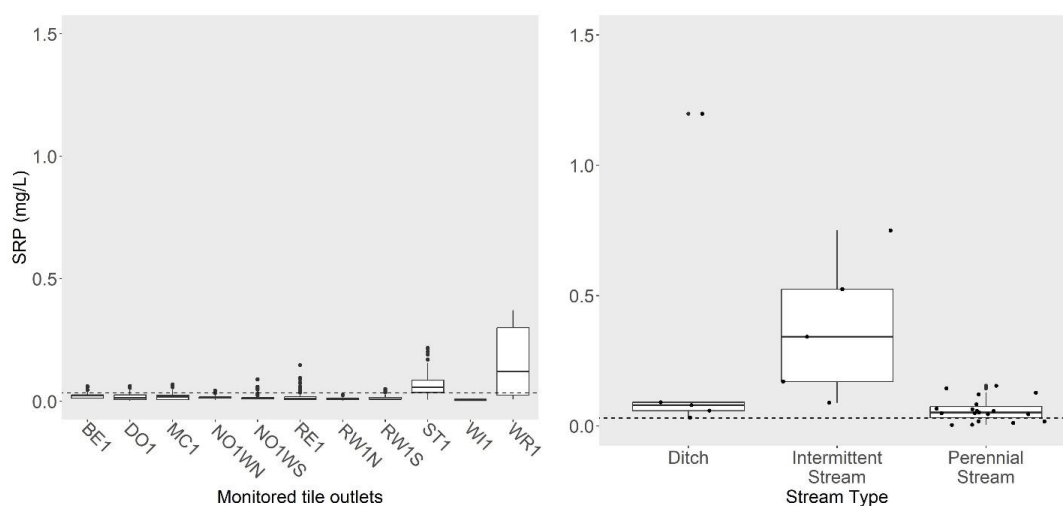
485

3.6 Low flow SRP concentrations from additional field sites

Among gaged stream and river sites, small order systems (especially first through third order ditches and streams) were under-represented relative to their prevalence across the landscape. These smaller order systems are also less



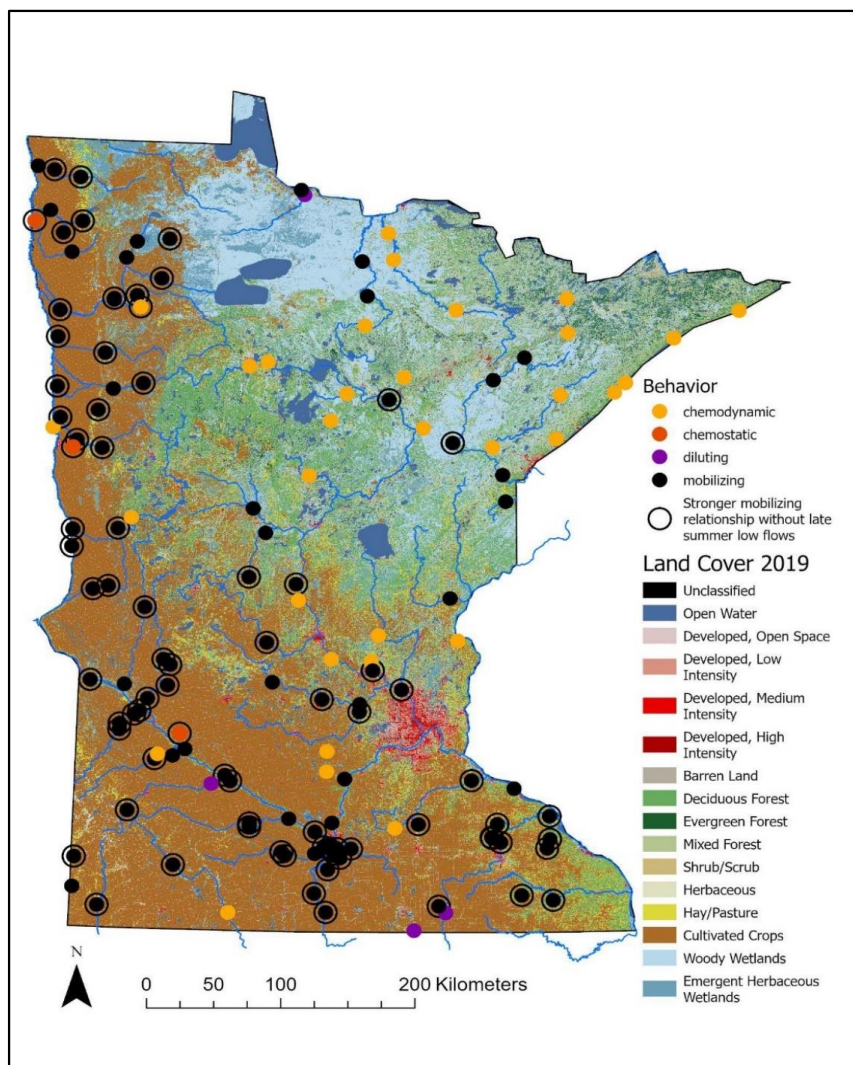
490 likely to have substantial point source discharges. To get a better understanding of SRP conditions in smaller order
 systems, we examined SRP concentrations collected from 33 agriculturally-dominated ditches, streams and mid-sized
 rivers in southern Minnesota during low flow conditions in August of 2014 (Dolph et al., 2017). During this sampling
 event, SRP concentrations at most sites were higher than mean SRP concentrations from farm tile outlets (Fig. 6).
 Mean SRP concentrations in late summer were highest in ditches (0.19 mg/L) and intermittent streams (0.19-0.30
 495 mg/L).



500 **Figure 6: SRP concentrations (mg/L) among tile outlets (left panel) compared to sampled ditches, intermittent streams and rivers, and perennial streams/rivers (right panel) during late summer low flow conditions. Dashed line shows mean SRP concentration for tile outlets in late summer.**

3.7 C-Q relationships at stream and river gages

When C-Q relationships were evaluated using all flow data for each gage, the majority of gaged watersheds (72%,
 n=103) showed mobilizing behavior for SRP in relation to stream flow (i.e., significant positive slopes for the C-Q
 505 power law relationship and $CV_C/CV_Q > 0.3$; Fig. A3). Mobilizing behavior for bioavailable P ranged from very weak
 ($R^2=0.01$) to comparatively strong ($R^2=0.68$). Watersheds with positive SRP-Q relationships were located
 predominantly in the agriculturally dominated regions of the state (the southern and western parts of the state
 corresponding to the southern part of the Upper Mississippi River Basin, the Minnesota River Basin, the Driftless
 areas in the southeast, and the Red River Basin; Fig. 7). Chemodynamic behavior (non-significant slopes for the C-Q
 510 power law relationship and $CV_C/CV_Q > 0.3$) was observed for 24% (n=34) of sites, most located in the central and
 northeastern parts of the state dominated by forest and wetland cover (Fig. 7). A small number of sites (n=4, 3%)
 showed diluting behavior for SRP, as defined by significant negative slopes for the C-Q power law relationship and
 $CV_C/CV_Q > 0.3$. Two of these sites showed considerable wastewater treatment plant influences (wastewater treatment
 plant density > 0.005 sites/km²; Table A3). Three sites (2%) showed chemostatic behavior for SRP transport, as defined
 515 by a $CV_C/CV_Q \leq 0.3$.



520

Figure 7: Transport behavior of SRP in relation to flow (Q) for gaged watersheds ($n=143$). Dots indicate gage locations. Color of dots indicates transport behavior diagnosed by slope b of the $C-Q$ power law relationship and CV_C/CV_Q . Mobilizing = black dots ($n=103$); Chemodynamic = light orange dots ($n=34$); Diluting = purple dots ($n=4$); Chemostatic = dark orange ($n=3$). Sites with a stronger mobilizing relationship (i.e., an increase in slope b) when late summer low flows were excluded are shown as open circles ($n=78$). Land cover is based on the 2019 National Land Cover Database.



When low flow samples from late summer were removed, 54% of gaged watersheds (n=78) exhibited an increase in the slope of the mobilizing relationship between SRP and Q (Fig. 7; Appendix Table A5). For these sites, slopes of the C-Q relationships increased by 23%, on average, after late summer low flow samples were excluded (range in percent slope increase was 0.1%-273%). In other words, mobilizing behavior for SRP was stronger when these late summer low flow conditions were excluded. Examples of this phenomenon for four different gaged watersheds are shown in Fig. 8, where the slope of the C-Q relationship is steeper when late summer low flow samples were excluded, and comparatively flatter when they are included. Watersheds where late summer low flows modulated (flattened) the slope of the C-Q relationship for SRP were again located predominantly in the agriculturally dominated regions of the state (Fig. 7).

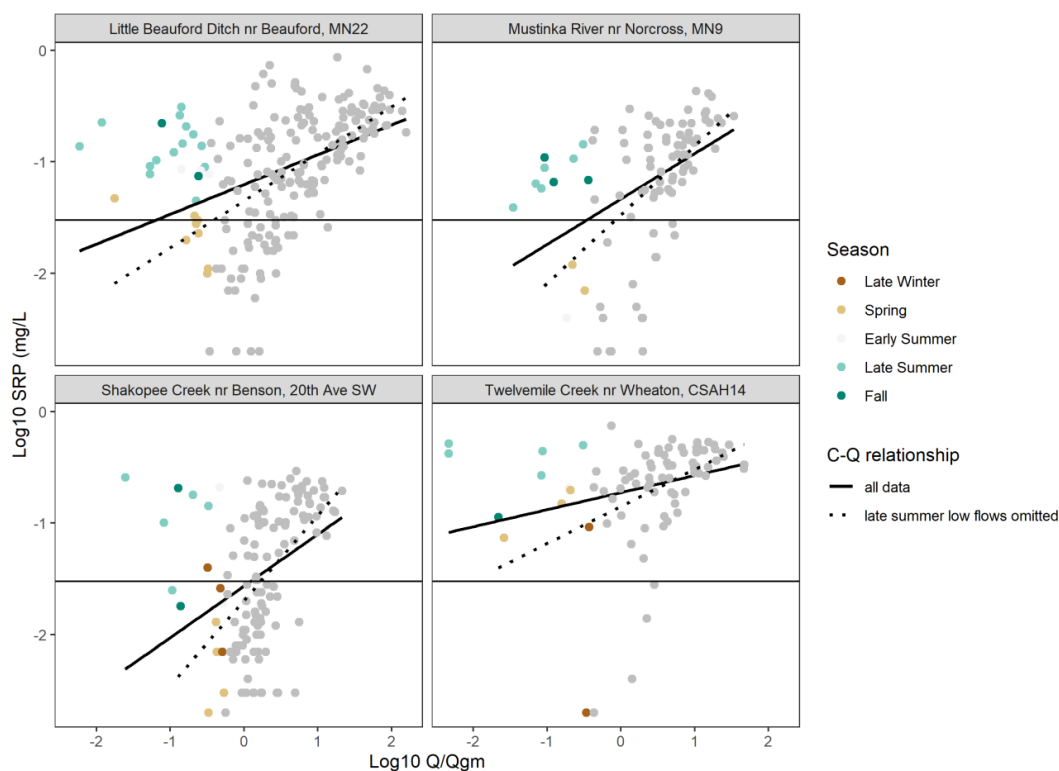


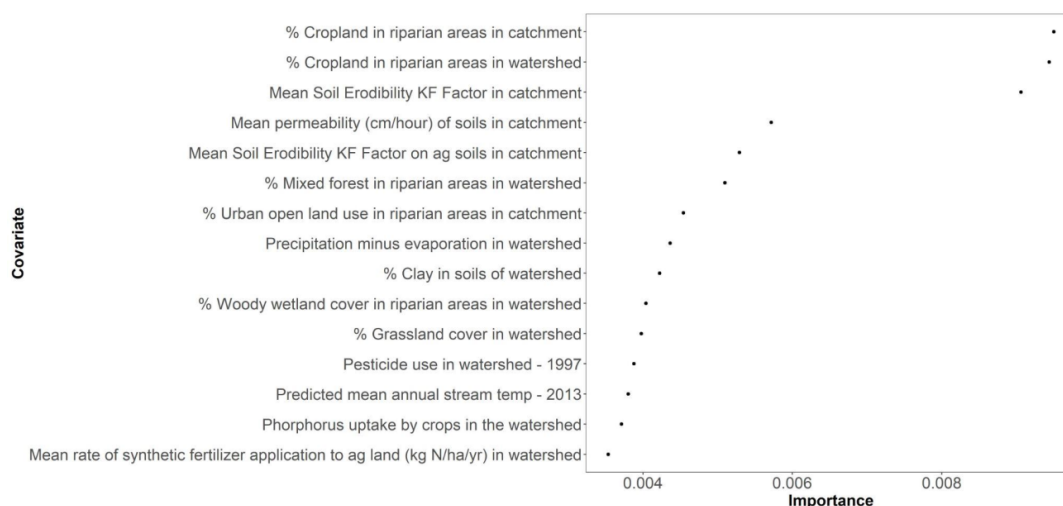
Figure 8: Example watersheds where low flows in late summer modulate the slope of the C-Q relationship for SRP. Low flow samples are shown as colored points where color indicates the season in which they were collected. All other samples are shown in gray. When all data are included, the slope of the overall C-Q relationship is reduced (solid line) compared to slopes for analyses with late summer low flow samples omitted(dashed line), indicating stronger mobilizing behavior.

3.8 Regression analysis to identify drivers of elevated SRP concentrations in late summer

The final selected hyperparameters for the random forest model based on model tuning with tenfold cross validation for this dataset were mtry = 7, trees = 1000, min_n = 6. Evaluation of predicted vs. actual late summer SRP for the independent test dataset indicated a model RMSE of 0.10, and an R² of 0.41 (Fig. A4). The top 15 predictors to model



performance are shown in Fig. 9. Importance values for all predictors are shown in Table A6. Partial dependence plots
 for these top predictors (Fig. 10) showed that higher SRP during late summer low flow conditions was associated
 545 with: higher cropland land use in riparian areas, various soil characteristics (higher soil erodibility, lower soil
 permeability, higher soil clay content), greater agricultural intensity (higher pesticide use, higher phosphorus uptake
 by crops, higher fertilizer application rates), more urban land use in riparian areas, lower woody wetland, and mixed
 forest in riparian areas, lower grassland land use in watersheds, lower surplus precipitation in the watershed
 (precipitation minus evaporation) and higher stream temperatures. Table 3 summarizes possible mechanisms linking
 550 these attributes to riverine SRP concentrations.



555 **Figure 9: Conditional Permutation Importance (CPI) values for the top 15 predictors in the random forest model for late summer SRP during low flows and stream and river gages. CPI is a measure that can be used to assess how much each variable ‘adds’ to accurately predicting the response variable, given what we know from all other covariates. Importance values for all attributes are given in Table A6.**

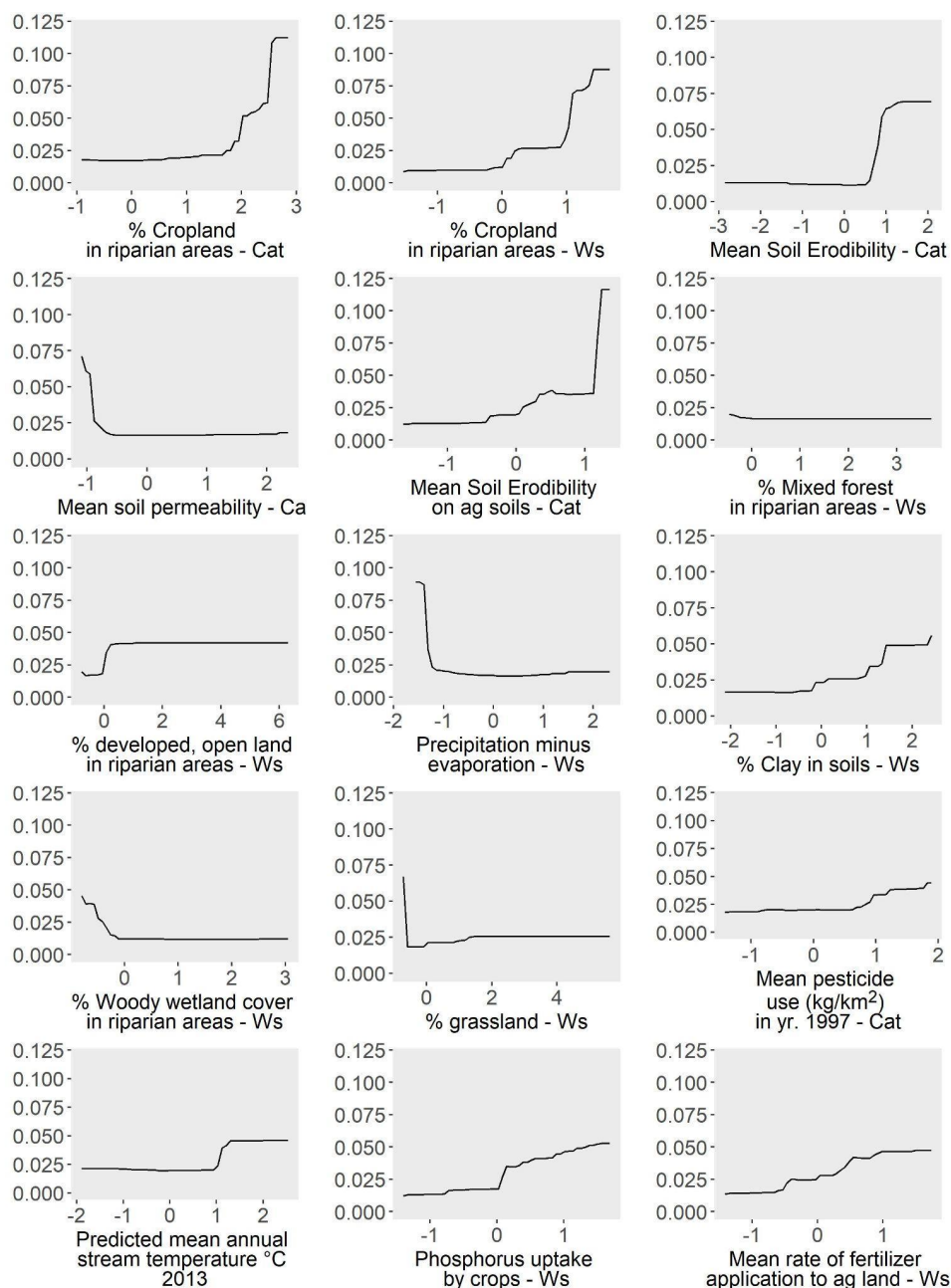


Figure 10: Partial dependence (y axis = change in predicted SRP value) for each of the 15 most important predictors to model performance. Partial dependence shows the change in the response variable (late summer low flow SRP) when each predictor of interest is varied while all other predictors stay constant. “Ws”=predictors summarized at watershed scale, “Ca”=predictors summarized at catchment scale. All predictor variables are from the U.S. EPA StreamCat dataset (Hill et al., 2016).

560



565

Table 3: Possible mechanisms linking random forest model predictor variables to late summer SRP concentrations during low flow conditions, for the top 15 attributes identified as most important to the performance of the random forest model. All attributes are from the U.S. EPA StreamCat dataset.

Attribute	Relationship	General mechanism category	Potential specific mechanism(s) linked to elevated late summer SRP
Percent of local NHD catchment classified as crop land use (NLCD 2019) within a 100-m buffer of NHD streams	Increasing SRP with increasing crop cover grown in proximity to river network	Direct inputs and/or legacy P supply	Indicator of current and historic P inputs from ag land use, especially in local riparian areas
Percent of watershed classified as crop land use (NLCD 2019) within a 100-m buffer of NHD streams	Increasing SRP with increasing crop cover grown in proximity to river network	Direct inputs and/or legacy P supply	Indicator of current and historic P inputs from ag land use, especially in local and upstream riparian areas
Mean soil erodibility factor (kffact, via STATSGO) within local NHD catchment; represents a relative index of susceptibility of bare, cultivated soil to particle detachment and transport by rainfall	Increasing SRP with increasing soil erodibility	Direct inputs and/or legacy P supply	Inputs of soil-associated P into river networks, either current or historic
Mean permeability (cm/hour) of soils (STATSGO) within local NHD catchment	Higher SRP at very low soil permeability	Mediates biogeochemical processes in near channel environment	Low permeability impedes oxygen exchange to the hyporheic zone, facilitating redox-mediated P release
Percent of watershed classified as mixed forest land cover (NLCD 2019) within a 100-m buffer of NHD streams	Higher SRP with low mixed forest cover in riparian areas	Direct inputs and/or legacy P and/or mediates biogeochemical processes	Fewer current or historic inputs of P to river networks with forested riparian areas; potential for forested riparian areas to trap P; shading of river channel alters stream productivity/stream metabolism
Percent of local NHD catchment classified as developed, open space land use (NLCD 2019) within a 100-m buffer of NHD streams	Higher SRP with higher open urban land use in riparian buffer	Direct inputs and/or legacy P supply	Indicator of urban land use and associated P inputs; could also mediate biogeochemical processes by altering stream temperature or flow conditions (i.e., higher stream temps in urban areas; stormwater infrastructure contributing to low flow conditions during dry periods, etc)
Precipitation (mm) minus potential evaporation within watershed	Higher SRP at low and high ends of precipitation range	Mediates biogeochemical processes in near	Dry conditions contribute to higher stream temperatures and lower discharge, influencing



		channel environment	biologically-mediated P release
Mean % clay content of soils within watershed	Higher SRP with greater clay content in soils	Mediates biogeochemical processes in near channel environment	Fe-containing clay sediments can adsorb P and release it via redox reactions
Percent of watershed classified as woody wetland land cover (NLCD 2019) within a 100-m buffer of NHD streams	Higher SRP with low woody wetland cover in riparian buffers	Mediates biogeochemical processes in near channel environment	Woody wetlands acting as sinks for SRP
Percent of local catchment classified as grassland/herbaceous land cover (NLCD 2019)	Higher SRP at low grassland cover	Direct inputs and/or legacy P supply	Fewer historic and ongoing P inputs in grasslands vs ag/urban lands
Mean pesticide use (kg/km ²) in yr. 1997 within watershed	Increasing SRP with increasing pesticide use	Direct inputs and/or legacy P supply	Indicator of agricultural intensity and degree of historic/current P inputs
Predicted mean annual stream temperature for 2013	Higher SRP with higher stream temperatures	Mediates biogeochemical processes in near channel environment; Proxy for direct inputs and/or legacy P supply	Indicator of temperature-mediated biological activity, or of land use differences across climate gradients associated with P inputs (e.g., more agriculture & associated legacy P supplies in warmer climates)
Phosphorus uptake by crops in the watershed	Increasing SRP with increasing P uptake	Direct inputs and/or legacy P supply	Indicator of agricultural intensity and degree of historic/current P inputs
Mean rate of synthetic nitrogen fertilizer application to agricultural land in kg N/ha/yr, within the watershed	Increasing SRP with increasing fertilizer inputs	Direct inputs and/or legacy P supply	Indicator of agricultural intensity and degree of historic/current P inputs



4 Discussion

In this study we observed that elevated concentrations of bioavailable P (i.e., SRP) were widespread among rivers and streams during late summer low flow conditions in Minnesota. Between one-third to one half of the gaged watersheds we studied exhibited SRP concentrations during late summer low flows that were above previously identified thresholds for eutrophication of 0.02 - 0.04 mg/L for freshwater environments (Zeng et al., 2016; Poikane et al., 2021; (34% were above a threshold of 0.04 mg/L and 53% of watersheds were above 0.02 mg/L). Just under half of gaged watersheds we studied (39%) also had SRP concentrations during late summer low flows that exceeded mean tile drainage SRP concentrations in the same season. Gaged watersheds exhibiting high late summer SRP concentrations during low flows were characterized by anthropogenically dominated landscapes (i.e., urban and/or agricultural land use); by contrast, watersheds with forest- and wetland-dominated landscapes exhibited low SRP concentrations during late summer low flows. One avenue for future research is to investigate how the timing and duration of elevated summer SRP concentrations affect local and downstream eutrophication outcomes. On the one hand, the large majority of annual P export by load likely occurs under high flow conditions in late winter and spring (Dolph et al., 2019; Schilling et al., 2020). However, the release of highly bioavailable P during hot, dry summer periods when conditions are optimal for algal growth in lakes and rivers may also drive increased eutrophication risk, resulting in outcomes such as increased occurrence of harmful algal blooms (Paerl and Huisman, 2008). As climate change results in increased prolonged periods of drought and heat during summers in the Upper Midwest, the effects of elevated bioavailable P at low flows could be extended for longer parts of the season.

We also observed that elevated SRP concentrations during low flow conditions in late summer altered apparent *C-Q* transport behavior for many streams and rivers in anthropogenically altered landscapes. For more than half of the gaged watersheds we studied (54%), elevated SRP concentrations during low flows in late summer dampened *C-Q* relationships which would have otherwise appeared more strongly mobilizing across other seasons and flow conditions. Strongly mobilizing relationships are indicative of landscape connectivity as a key driver for SRP export (Musloff et al., 2015), with flow accumulation and riparian areas identified as critical source areas for SRP (Casquin et al., 2021; Dupas et al., 2023). Thus, for many of the sites we studied, connectivity appears important to SRP export during winter, spring and early summer and during moderate to high flow conditions at all times of year. During late summer low flows, by contrast, other in-channel dynamics may cause riverine *C-Q* patterns to deviate from linear relationships (Meybeck and Moatar, 2012). Below we discuss possible mechanisms that may contribute to comparatively high SRP concentrations during late summer low flow conditions in streams and rivers of our study region.

4.1 Drivers of SRP during late summer low flows

We hypothesized that elevated riverine SRP concentrations during late summer low flows could arise from 1) point sources (i.e., wastewater treatment discharges), 2) tile drainage or 3) biogeochemical processes that release legacy P. Overall, our analysis shows that landscape drivers that govern diffuse P inputs and legacy P supply in the river network, as well as wastewater inputs and biogeochemical processes, are associated with high late summer SRP concentrations during low flows at many anthropogenically-dominated sites. Table 3 summarizes attributes that were



most important to predicting late summer SRP concentrations in our random forest model and identifies whether these attributes are most likely related to historic and current P inputs (and therefore legacy P supply) or to processes that mediate the storage and release of P from the river channel. Wastewater treatment plant density did not rank among the most important predictors to model performance. However, the influence of wastewater on summer low flow SRP was evident in elevated SRP concentrations at sites with strong wastewater influence throughout most seasons (apart from spring, when low flow SRP concentrations were nearly universally low, presumably due to rapid in-stream uptake or abiotic immobilization). We also observed direct (though weak) correlations with low flow SRP in late summer and wastewater treatment plant density in gaged watersheds.

Several lines of evidence suggest that wastewater influences were not solely responsible for elevated riverine SRP concentrations during late summer low flow conditions. First, 38% of the streams and rivers we studied exhibited elevated SRP concentrations (above 0.02 mg/L) during late summer low flow conditions despite having limited or no wastewater treatment plant influence in their watersheds. Second, we also identified a number of land use attributes that were more important to predicting late summer low flow SRP. Crop cover was strongly and directly related to SRP concentrations during low flow conditions in all seasons, and crop cover in riparian areas at the local catchment and watershed scales were the top two most important variables to the performance of the random forest model used to predict late summer low flow SRP concentrations. Other top variables to model performance included aspects of agricultural intensity at the watershed or catchment scale (pesticide use, phosphorus uptake by crops, and fertilizer application), as well as urban land use in riparian areas. The importance of these variables points to historic and ongoing inputs of P arising from intensive/industrial agriculture and urban land use that have resulted in the accumulation of legacy P in riverine channels, which can potentially be released under environmental conditions such as warm temperatures, low oxygen and variable moisture. Conversely, greater mixed forest or woody wetland land use in riparian areas was associated with lower SRP concentrations during late summer low flows, perhaps because these environments may act as sinks for bioavailable P (Ury et al., 2023). Overall, it is notable that land use in riparian areas showed up as top variables of importance to model performance, suggesting that near channel environments (and therefore potentially near channel management practices) may be important in regulating elevated SRP during late summer low flows. Lastly, both geologic and climatic variables (soil erodibility, soil permeability, clay content of soils, mean winter stream temperatures, and precipitation minus evaporation) were also identified as important in the random forest model predicting late summer low flow SRP, suggesting that environmental factors which mediate biogeochemical processes also likely play an important role in driving late summer riverine SRP concentrations.

Interestingly, SRP concentrations during late summer low flow conditions in anthropogenically-dominated watersheds often exceeded tile SRP concentrations. Although tile drainage is known to represent a key input of P to river networks (Smith et al., 2015), it may be that in-channel dynamics beyond tile concentrations drive variability in SRP concentration during summer low flows. However, it is also important to note that the two tile outlets draining farms with dairy operations exhibited much higher SRP concentrations during late summer (and all times of year), compared to tile outlets draining fields characterized only by corn and soybean row crops. Thus, the prevalence of CAFOs and other animal agriculture operations is likely to strongly influence the contribution of tile drainage to riverine SRP concentrations. Three sites also had a surface inlet to their tile drainage system. These tile systems had comparatively



640 high SRP during winter, spring or early summer (depending on the site), which can likely be explained by the additional loss of sediment and nutrients to surface inlets during snowmelt on frozen and thawing soils (Feyereisen et al., 2015). However, the two surface inlet-influenced sites without dairy operations exhibited SRP concentrations during late summer similar to other nondairy impacted sites.

4.2 Biogeochemical processes and riverine SRP

645 Previous studies have identified a number of biogeochemical processes that can affect riverine concentrations of SRP at low flows. These processes include: 1) the concentration of legacy P entering the stream via groundwater and/or streambed pore water, 2) redox-driven release of P from stream sediments, and 3) release of P resulting from mineralization of organic matter.

650 During low flow conditions, groundwater and/or pore water can become proportionately dominant components of flow, with stores of legacy P in these sources contributing more strongly to overall riverine SRP. These groundwater sources can include tile drainage (Schilling et al., 2020; Rode et al., 2023), but can also include streambed pore water entering from the hyporheic zone via upwelling flow paths with P concentrations that are distinct and potentially higher than that of tile drainage (Vissers et al., 2023). Upwelling of P-rich pore water can be patchy and is likely controlled by hyper-local spatial and temporal conditions operating at the reach scale, such as the availability and extent of reducing vs oxic conditions (e.g., Vissers et al., 2023).

655 SRP can also be released into river channels from stream sediments. Stream sediments often have the potential to buffer stream SRP concentrations by adsorbing P (Simpson et al., 2021). However, this buffering capacity will depend on sediment and stream characteristics, including sorption affinity, stream pH, exchangeable P concentration, sediment particle sizes, and seasonal variation in temperature, light, discharge, redox, primary productivity, stream respiration and sediment inputs (Simpson et al., 2021). Seasonal release of SRP is commonly thought to occur via the reduction of Fe-, Mn- or Al- oxyhydroxide-containing sediments under anoxic conditions, releasing PO_4^{3-} . These anoxic conditions typically arise when flow velocities are low, water and sediment temperatures increase, and oxygen becomes depleted due to increased microbial activity. For example, Smolders et al., (2017) showed that high summer concentrations of bioavailable P for rivers in Belgium was likely explained by internal loading from legacy P that was released from sediments when dissolved oxygen concentrations were low and P:Fe molar ratios in sediment were large.

665 Lastly, Jarvie et al., (2020) showed that, in a wetland-pond system, microbial respiration and the resulting mineralization of organic matter can also represent a source of bioavailable P under low flow conditions in summer and fall. They found that SRP release was potentially related to drier and hotter conditions that could facilitate both higher rates of biomass accumulation and its subsequent breakdown via microbial processes. Presumably, this dynamic could also be at play for slow moving ditches and streams in parts of our study region, where water is sometimes nearly stagnant in summer. Under low flow conditions and warm temperatures, ditches and streams may operate in ways that are similar to wetlands or other lentic water bodies. The stream network is also populated with in-channel and riparian wetlands that may further affect ambient SRP concentrations. Felton et al. (2023) found 670 elevated dissolved P concentrations along a longitudinal stream gradient where the channel intersected wetlands and



concluded that locally elevated SRP could reflect P release from decomposition of organic matter in wetland environments; however in that study elevated P concentrations did not persist downstream and were assumed to be rapidly assimilated or adsorbed to sediments.

680 Our findings provide some insight as to the relative importance of these potential in-channel processes in determining
seasonally elevated SRP concentrations at low flow. The importance of climate and geologic variables in the random
forest model we used to predict late summer low flow SRP suggests that characteristics of stream sediments and/or
climate-mediated biotic activity may play an important role in elevated SRP concentrations in late summer. Partial
dependence plots indicated that increased SRP during late summer low flows was associated with the drier conditions
685 (lower precipitation minus evaporation in gaged watersheds) and warmer conditions (higher predicted mean stream
temperatures)⁹. This finding could be consistent with an important role for biologically-mediated processes such as
microbial respiration that are affected by temperature and stream discharge. Microbial activity is important both in the
decomposition of organic matter (i.e., mineralization), as well as in the reduction of redoximorphic sediments (i.e.,
sediments containing Fe, Al, Mn, etc), both of which can result in the release of SRP. The predicted mean stream
temperature values used in this study were derived from Hill et al. (2013), and were themselves influenced by air
690 temperature, soil permeability, agricultural and urban land use, stream slope, the influence of reservoirs, and watershed
area. The positive relationship between stream temperature and late summer SRP at low flow needs further
investigation, but could also be related to greater influence of groundwater or to climate gradients that correspond to
variation in biological activity or in land use and associated P inputs.

Soil erodibility was also identified as one of the most important variables to random forest model performance, with
695 partial dependence plots showing higher SRP during late summer low flows corresponding with greater soil erodibility
in the local catchment. Eroded soils have long been understood as a primary vector by which P enters river networks
(Berhe et al., 2018). Recently, this understanding has expanded to include eroded stream bank sediments as an
additional driver of downstream P transport (Margenot et al., 2023). Sediment-associated P may be temporarily stored
in river channels, with desorption of P occurring under certain environmental conditions, as described above.

700 Partial dependence plots showed that late summer low flow SRP concentrations were highest where soil permeability
of soils in local catchments was low. This finding is also consistent with release of P from stream sediments. Low soil
permeability is characteristic of fine sediments (Ren and Santamarina, 2018). If broader watershed soil types are
indicative of in-stream sediment, very low permeability of fine grained stream sediments could impede oxygen
exchange to the hyporheic zone, potentially creating anoxic conditions to facilitate redox-mediated P release
705 (Mendoza-Lera and Datry, 2017).

Partial dependence plots also indicated that increased SRP during late summer low flow conditions was associated
with increased clay content of soils in gaged watersheds. Clay particles are small in size, providing greater P adsorption

⁹ Note that stream temperature data in the U.S. EPA StreamCat dataset is derived from Hill et al. (2013) and takes into account natural factors and certain aspects of anthropogenic influence (i.e., reservoirs, urban land use and agricultural land use) but does not account for wastewater effluent.



potential (Simpson et al., 2021). However, the deposition of fine clay sediments can also affect hyporheic exchange and organic matter processing (Simpson et al., 2021). Clay sediments also typically contain iron (Fe) that can bind P and can therefore provide a substrate for microbially mediated redox reactions (Pentrakova et al., 2013). Our findings are consistent with a mechanism whereby clay sediments bind considerable P under some conditions, and then release it via redox reactions during late summer when oxic conditions are low due to microbial decomposition of organic matter.

Environmental conditions in large parts of our study region are consistent with those previously reported to foster situational SRP release from sediments. Previous studies have observed release of SRP from stream sediments when SRP to Fe ratios in sediments are high and when dissolved oxygen concentrations are low (Inamdar et al., 2020; van Dael et al., 2020; Diamond et al., 2023). These conditions are characteristic of slow moving lowland streams with large legacy P stores arising from current and historic P inputs, and may be especially common in headwater streams (Diamond et al., 2023). Such conditions are widespread across our study region. Ditches, streams, and rivers in the flat to gently rolling landscapes of southern and northwestern Minnesota are characterized by relatively low gradients, high current and historic P loading from agriculture and urban land use (Boardman et al., 2019), and high rates of instream primary productivity (Dolph et al., 2017b). These conditions are likely to coincide during warm late summer conditions in high rates of microbial respiration, anoxic conditions, and P release.

Overall, our findings agree with previous studies that have identified the importance of biogeochemical processes in seasonally modulating nutrient concentrations during low flows in lowland lotic systems (e.g., Smolders et al., 2017) and in many ways parallels findings for eutrophic lakes (Søndergaard et al., 2001). Further study is needed to parse the importance of pore water, stream sediment dynamics, and mineralization to the elevated SRP concentrations we observed at various stream and river sites during late summer low flow conditions. It is also important to note that performance of the random forest model in predicting late summer SRP concentrations was middling ($R^2=0.41$). We speculate that improved model performance will depend on reach-scale variables that may strongly determine SRP dynamics, such as channel morphology, characteristics and volume of bed sediment, and stream productivity and respiration. Future research could aim to incorporate both reach scale and broader scale variables into a more precise understanding of in channel SRP dynamics. For example, the sampling platform described by Felton et al. (2023) presents the intriguing possibility of monitoring stream conditions intensively along longitudinal gradients and could be refined to include measures of dissolved oxygen, CO_2 (as a proxy for respiration), temperature, sorption capacity, and/or to identify P inputs associated with tile and point discharges or certain aspects of channel morphology.

5 Conclusions

In this study we observed widespread elevation of SRP concentrations during late summer low flow conditions among anthropogenically-dominated ditches, streams and rivers in Minnesota. As summers become hotter and drier – predicted climate changes in our region – conditions for the release of legacy P stored in stream and river channels will likely become more prolonged and/or more acute, contributing to the increased occurrence of adverse events such as harmful algal blooms. Further study is needed to determine the duration, fate and dominant mechanisms associated with riverine release of bioavailable P during late summer and other times of year.



745 We found that elevated riverine concentrations of SRP during low flow conditions in late summer altered *C-Q*
transport behavior for more than half (54%) of the gaged watersheds we studied, weakening what was otherwise more
strongly mobilizing behavior during higher flow conditions and other times of year. These watersheds occurred almost
exclusively in landscapes that were heavily modified by agricultural or urban land use.

750 We found that while wastewater discharge likely contributed to elevated SRP concentration at low flow for some sites,
most sites exhibiting elevated SRP concentrations during late summer low flow conditions did not have substantial
wastewater treatment impacts. Moreover, elevated SRP concentrations during low flow at these sites typically
exceeded tile drainage SRP concentrations from corn and soy planted farm fields during late summer. We found that
SRP concentrations during late summer low flow conditions were related to land use (cropland land use in riparian
areas, mixed forest land use in riparian areas, woody wetland land use in riparian areas, urban land use in riparian
755 (higher pesticide use, higher phosphorus uptake by crops, higher fertilization rates), and climate (watershed
precipitation and stream temperature). Taken together, these findings suggest that climate and geologically mediated-
biogeochemical processes likely result in the release of in-channel stores of legacy P during late summer low flow
conditions in a substantial number of stream and river sites that have been heavily impacted by past and current P
inputs associated with industrial/intensive agriculture and urbanization. Our findings suggest that efforts to reduce the
760 impacts of bioavailable P to freshwaters will need to address both 1) mobilization of dissolved P from the landscape
during high flow conditions and 2) in-channel environments that result in the release of accumulated legacy P from
streams and rivers during summer low flows when freshwater systems are especially vulnerable to eutrophication
outcomes. With regards to management, the association of land use in riparian areas with SRP during late summer
low flows suggests that practices targeting near channel and riparian environments may be important in regulating
765 elevated SRP in these conditions. Controlling ongoing P inputs will also be instrumental to reducing riverine P loading.
For example, in Minnesota, additional phosphorus regulations added to National Pollutant Discharge Elimination
System (NPDES) permits since the year 2000 have resulted in substantial reductions of P loading arising from
wastewater facilities¹⁰. Policies and management approaches to substantially reduce inputs of fertilizer, manure and
wastewater, as well their losses via surface, tile and other groundwater pathways, remain critical to achieving societal
770 water quality goals.

Code availability

All R scripts used for data analysis are available from https://github.com/cldolph/instream_legacyP

Data availability

775 All input data used in this paper are available from https://github.com/cldolph/instream_legacyP

Author contribution

780 CD, BD, GF and JF conceived study design, identified available datasets, and identified research questions. CD
performed data analysis and developed R scripts. CD prepared the manuscript with contributions from all co-authors.

¹⁰ <https://www.pca.state.mn.us/business-with-us/phosphorus-in-wastewater>



Competing interests

The authors declare that they have no conflict of interest.

Acknowledgements

785 This project was supported through the U.S. Department of Agriculture's Conservation Effects Assessment Project (CEAP) National Legacy Phosphorus Assessment, with funding provided by USDA Natural Resources Conservation Service (NRCS) through an Interagency Agreement (Agreement # NRC21IRA0010879). CEAP (<https://www.nrcs.usda.gov/ceap>) is a multi-agency effort led by the Natural Resources Conservation Service and the Agricultural Research Service to quantify the effects of voluntary conservation and strengthen data-driven
790 management decisions across the nation's private lands.

References

- 795 Basu, N.B., Destouni, G., Jawitz, J.W., Thompson, S.E., Loukinova, N.V., Darracq, A., Zanardo, S., Yaeger, M., Sivapalan, M., Rinaldo, A., and Rao, P.S.C.: Nutrient loads exported from managed catchments reveal emergent biogeochemical stationarity, *Geophysical Research Letters*, 37, <https://doi.org/10.1029/2010gl045168>, 2010.
- Bennett, E.M., Carpenter, S.R., and Caraco, N.F.: Human Impact on Erodable Phosphorus and Eutrophication: A Global Perspective, *BioScience*, 51, 227. [https://doi.org/10.1641/0006-3568\(2001\)051\[0227:hioepa\]2.0.co;2](https://doi.org/10.1641/0006-3568(2001)051[0227:hioepa]2.0.co;2), 2001.
- 800 Berhe, A.A., Barnes, R.T., Six, J., and Marín-Spiotta, E.: Role of Soil Erosion in Biogeochemical Cycling of Essential Elements: Carbon, Nitrogen, and Phosphorus, *Annual Review of Earth and Planetary Sciences*, 46, 521–548. <https://doi.org/10.1146/annurev-earth-082517-010018>, 2018.
- 805 Bierzo, M.Z. and Heathwaite, A.L.: Seasonal variation in phosphorus concentration–discharge hysteresis inferred from high-frequency in situ monitoring, *Journal of Hydrology*, 524, 333–347, <https://doi.org/10.1016/j.jhydrol.2015.02.036>, 2015.
- Boardman, E., Danesh-Yazdi, M., Fofoula-Georgiou, E., Dolph, C.L., and Finlay, J.C.: Fertilizer, landscape features and climate regulate phosphorus retention and river export in diverse Midwestern watersheds, *Biogeochemistry*, 146, 293–309, <https://doi.org/10.1007/s10533-019-00623-z>, 2019.
- 810 Casquin, A., Gu, S., Dupas, R., Petitjean, P., Gruau, G., and Durand, P.: River network alteration of C-N-P dynamics in a mesoscale agricultural catchment, *Science of The Total Environment*, 749, 141551, <https://doi.org/10.1016/j.scitotenv.2020.141551>, 2020.
- Debeer D, Hothorn T, and Strobl C: `permimp`: Conditional Permutation Importance, R package version 1.0-2, <https://CRAN.R-project.org/package=permimp>, 2021.
- 815 Dewitz, J.: National Land Cover Database (NLCD) 2019 Products [Data set], U.S. Geological Survey. <https://doi.org/10.5066/P9KZCM54>, 2021.
- Diamond, J.S., Moatar, F., Recoura-Massaquant, R., Chaumot, A., Zarnetske, J., Valette, L., and Pinay, G.: Hypoxia is common in temperate headwaters and driven by hydrological extremes, *Ecological Indicators*, 147, 109987. <https://doi.org/10.1016/j.ecolind.2023.109987>, 2023.
- 820 Dolph, C.L.; Hansen, A.T.; Kemmitt, K. L.; Janke, B.; Rorer, M.; Winikoff, S., et al.: Characterization of streams and rivers in the Minnesota River Basin Critical Observatory: Water chemistry and biological field collections, 2013–2016, Retrieved from the Data Repository for the University of Minnesota, <https://doi.org/10.13020/D6FH44>, 2017a.
- 825 Dolph, C. L., Hansen, A. T., and Finlay, J. C.: Flow-related dynamics in suspended algal biomass and its contribution to suspended particulate matter in an agricultural river network of the Minnesota River Basin, USA, *Hydrobiologia*, 785(1), 127–147, <http://doi.org/10.1007/s10750-016-2911-7>, 2017b.
- Dolph, C.L., Boardman, E., Danesh-Yazdi, M., Finlay, J.C., Hansen, A.T., Baker, A.C., and Dalzell, B.: Phosphorus Transport in Intensively Managed Watersheds, *Water Resources Research*, 55, 9148–9172, <https://doi.org/10.1029/2018wr024009>, 2019.



- 830 Dolph, C.L., Cho, S.J., Finlay, J.C., Hansen, A.T., Dalzell, B.: Predicting high resolution total phosphorus concentrations for soils of the Upper Mississippi River Basin using machine learning, *Biogeochemistry*, 163, 289–310. <https://doi.org/10.1007/s10533-023-01029-8>, 2023.
- Dupas, R., Casquin, A., Durand, P., and Viaud, V.: Landscape spatial configuration influences phosphorus but not nitrate concentrations in agricultural headwater catchments, *Hydrological Processes*, 37, <https://doi.org/10.1002/hyp.14816>, 2023.
- 835 ESRI: ArcGIS Pro version 3.0.3. Redlands, CA: Environmental Systems Research Institute, 2022.
- Felton, R., Dalzell, B.J., Baker, J., Flynn, K.D., and Porter, S.A.: Novel, Ultralight Platform for Mapping Water Quality Parameters in Low-Order Streams, *ACS ES&T Water* 3, 3305–3314, <https://doi.org/10.1021/acsestwater.3c00280>, 2023.
- 840 Feyereisen, G.W., Francesconi, W., Smith, D.R., Papiernik, S.K., Krueger, E.S., and Wentz, C.D.: Effect of Replacing Surface Inlets with Blind or Gravel Inlets on Sediment and Phosphorus Subsurface Drainage Losses, *Journal of Environmental Quality*, 44, 594–604, <https://doi.org/10.2134/jeq2014.05.0219>, 2015.
- Godsey, S.E., Kirchner, J.W., and Clow, D.W.: Concentration-discharge relationships reflect chemostatic characteristics of US catchments, *Hydrological Processes*, 23, 1844–1864, <https://doi.org/10.1002/hyp.7315>, 2009.
- 845 Goyette, J.-O., Bennett, E.M., and Maranger, R.: Low buffering capacity and slow recovery of anthropogenic phosphorus pollution in watersheds, *Nature Geoscience*, 11, 921–925, <https://doi.org/10.1038/s41561-018-0238-x>, 2018.
- Greenwell, B.M.: pdp: An R Package for Constructing Partial Dependence Plots, *The R Journal*, 9, 421, <https://doi.org/10.32614/rj-2017-016>, 2017.
- 850 Hagenauer, J., Omrani, H., and Helbich, M.: Assessing the performance of 38 machine learning models: the case of land consumption rates in Bavaria, Germany, *International Journal of Geographical Information Science*, 33, 1399–1419, <https://doi.org/10.1080/13658816.2019.1579333>, 2019.
- Haque, S.E.: How Effective Are Existing Phosphorus Management Strategies in Mitigating Surface Water Quality Problems in the U.S.?, *Sustainability*, 13, 6565, <https://doi.org/10.3390/su13126565>, 2021.
- 855 Hill, R.A., Hawkins, C.P., and Carlisle, D.M.: Predicting thermal reference conditions for USA streams and rivers, *Freshwater Science*, 32, 39–55, <https://doi.org/10.1899/12-009.1>, 2013.
- Hill, R.A., Weber, M.H., Leibowitz, S.G., Olsen, A.R., and Thornbrugh, D.J.: The Stream-Catchment (StreamCat) Dataset: A Database of Watershed Metrics for the Conterminous United States, *Journal of the American Water Resources Association (JAWRA)*, 52, 120–128, <https://doi.org/10.1111/1752-1688.12372>, 2016.
- 860 Inamdar, S., Sienkiewicz, N., Lutgen, A., Jiang, G., and Kan, J.: Streambank Legacy Sediments in Surface Waters: Phosphorus Sources or Sinks?, *Soil Systems*, 4, 30, <https://doi.org/10.3390/soilsystems4020030>, 2020.
- Jarvie, H.P., Pallett, D.W., Schäfer, S.M., Macrae, M.L., Bowes, M.J., Farrand, P., Warwick, A.C., King, S.M., Williams, R.J., Armstrong, L., Nicholls, D.J.E., Lord, W.D., Rylett, D., Roberts, C., and Fisher, N.: 865 Biogeochemical and climate drivers of wetland phosphorus and nitrogen release: Implications for nutrient legacies and eutrophication risk, *Journal of Environmental Quality*, 49, 1703–1716, <https://doi.org/10.1002/jeq2.20155>, 2020.
- Johnson, L., Will Bartsch, George Hudak, Mae Davenport, Kris Johnson, Kristi Nixon, Jane Reed and Atlas Team: Minnesota Natural Resource Atlas: Online mapping tools and data for natural resource planning, management, and research in Minnesota, Natural Resources Research Institute, University of Minnesota Duluth, <https://mnatlas.org/>, 2022.
- 870 Keiser, D., and Shapiro, J.: Consequences of the Clean Water Act and the Demand for Water Quality, *The Quarterly Journal of Economics*, Volume 134, Issue 1, February 2019, 349–396, <https://doi.org/10.1093/qje/qjy019>, 2018.
- 875 King, K.W., Williams, M.R., and Fausey, N.R.: Contributions of Systematic Tile Drainage to Watershed-Scale Phosphorus Transport, *Journal of Environmental Quality*, 44, 486–494, <https://doi.org/10.2134/jeq2014.04.0149>, 2015.



- 880 Kreiling, R.M., Perner, P.M., Breckner, K.J., Williamson, T.N., Bartsch, L.A., Hood, J.M., Manning, N.F., and Johnson, L.T.: Watershed- and reach-scale drivers of phosphorus retention and release by streambed sediment in a western Lake Erie watershed during summer, *Science of The Total Environment*, 863, 160804, <https://doi.org/10.1016/j.scitotenv.2022.160804>, 2023.
- Liaw, A., and Wiener, M.: Classification and Regression by randomForest, *R News* 2(3), 18–22, 2002.
- 885 Margenot, A.J., Zhou, S., McDowell, R., Hebert, T., Fox, G., Schilling, K., Richmond, S., Kovar, J.L., Wickramaratne, N., Lemke, D., Boomer, K., and Golovay, S.: Streambank erosion and phosphorus loading to surface waters: Knowns, unknowns, and implications for nutrient loss reduction research and policy, *Journal of Environmental Quality*, 52, 1063–1079, <https://doi.org/10.1002/jeq2.20514>, 2023.
- Mayer, M.: `_missRanger: Fast Imputation of Missing Values_`. R package version 2.2.1, <https://CRAN.R-project.org/package=missRanger>, 2023.
- 890 MDA: MDA Discovery Farms Program field data and sample collection SOP. Minnesota Department of Agriculture, St. Paul, Minnesota. https://discoveryfarmsmn.org/wp-content/uploads/2021/07/DFM_Monitoring-SOP_v5_signed_Final.pdf, 2021.
- Mendoza-Lera, C., and Datry, T.: Relating hydraulic conductivity and hyporheic zone biogeochemical processing to conserve and restore river ecosystem services, *Science of The Total Environment*, 579, 1815–1821, <https://doi.org/10.1016/j.scitotenv.2016.11.166>, 2017.
- 895 Meybeck, M., and Moatar, F.: Daily variability of river concentrations and fluxes: indicators based on the segmentation of the rating curve, *Hydrological Processes*, 26, 1188–1207, <https://doi.org/10.1002/hyp.8211>, 2011.
- Minnesota Department of Natural Resources and Minnesota Pollution Control Agency: DNR/MPCA Cooperative Stream Gaging Locations, Available from: <https://gisdata.mn.gov/dataset/env-wiski-coop-stream-gaging> [Accessed January 30, 2023], 2023.
- 900 MPCA: Watershed Pollutant Load Monitoring Network (WPLMN) standard operating procedures and guidance: Surface water quality sampling, Minnesota Pollution Control Agency, St. Paul, Minnesota, <https://www.pca.state.mn.us/sites/default/files/wq-cml-02.pdf>, 2015.
- MPCA: Proposed impaired waters list. Minnesota Pollution Control Agency, St. Paul, Minnesota, <https://www.pca.state.mn.us/air-water-land-climate/minnesotas-impaired-waters-list>, 2022.
- 905 Musolff, A., Schmidt, C., Selle, B., and Fleckenstein, J.H.: Catchment controls on solute export, *Advances in Water Resources*, 86, 133–146, <https://doi.org/10.1016/j.advwatres.2015.09.026>, 2015.
- Osterholz, W.R., Hanrahan, B.R., and King, K.W.: Legacy phosphorus concentration–discharge relationships in surface runoff and tile drainage from Ohio crop fields, *Journal of Environmental Quality*, 49, 675–687, <https://doi.org/10.1002/jeq2.20070>, 2020.
- 910 Paerl, H.W., and Huisman, J.: Blooms Like It Hot, *Science*, 320, 57–58, <https://doi.org/10.1126/science.1155398>, 2008.
- Pentráková, L., Su, K., Pentrák, M., and Stucki, J.W.: A review of microbial redox interactions with structural Fe in clay minerals, *Clay Minerals*, 48, 543–560, <https://doi.org/10.1180/claymin.2013.048.3.10>, 2013.
- 915 Poikane, S., Várbró, G., Kelly, M.G., Birk, S., and Phillips, G.: Estimating river nutrient concentrations consistent with good ecological condition: More stringent nutrient thresholds needed, *Ecological Indicators*, 121, 107017, <https://doi.org/10.1016/j.ecolind.2020.107017>, 2021.
- R Core Team (2023). `_R: A Language and Environment for Statistical Computing_`, R Foundation for Statistical Computing, Vienna, Austria, <https://www.R-project.org/>
- 920 Records, R.M., Wohl, E., and Arabi, M.: Phosphorus in the river corridor, *Earth-Science Reviews*, 158, 65–88, <https://doi.org/10.1016/j.earscirev.2016.04.010>, 2016.
- Ren, X.W., and Santamarina, J.C.: The hydraulic conductivity of sediments: A pore size perspective, *Engineering Geology*, 233, 48–54, <https://doi.org/10.1016/j.enggeo.2017.11.022>, 2018.
- 925 Rode, M., Tittel, J., Reinstorf, F., Schubert, M., Knöller, K., Gilfedder, B., Merensky-Pöhlein, F., and Musolff, A.: Seasonal variation and release of soluble reactive phosphorus in an agricultural upland headwater in central



- Germany, *Hydrology and Earth System Sciences*, 27, 1261–1277, <https://doi.org/10.5194/hess-27-1261-2023>, 2023.
- Schilling, K.E., Streeter, M.T., Vogelgesang, J., Jones, C.S., and Seeman, A.: Subsurface nutrient export from a cropped field to an agricultural stream: Implications for targeting edge-of-field practices, *Agricultural Water Management*, 241, 106339, <https://doi.org/10.1016/j.agwat.2020.106339>, 2020.
- 930 Siebers, N., Kruse, J., Jia, Y., Lennartz, B., and Koch, S.: Loss of subsurface particulate and truly dissolved phosphorus during various flow conditions along a tile drain–ditch–brook continuum, *Science of The Total Environment*, 866, 161439, <https://doi.org/10.1016/j.scitotenv.2023.161439>, 2023.
- Simpson, Z.P., McDowell, R.W., Condon, L.M., McDaniel, M.D., Jarvie, H.P., and Abell, J.M.: Sediment phosphorus buffering in streams at baseflow: A meta-analysis, *Journal of Environmental Quality*, 50, 287–311, <https://doi.org/10.1002/jeq2.20202>, 2021.
- 935 Søndergaard, M., Jensen, P.J., and Jeppesen, E., Retention and Internal Loading of Phosphorus in Shallow, Eutrophic Lakes, *The Scientific World JOURNAL*, 1, 427–442, <https://doi.org/10.1100/tsw.2001.72>, 2001.
- Smith, D.R., King, K.W., Johnson, L., Francesconi, W., Richards, P., Baker, D., and Sharpley, A.N.: Surface Runoff and Tile Drainage Transport of Phosphorus in the Midwestern United States, *Journal of Environmental Quality*, 44, 495–502, <https://doi.org/10.2134/jeq2014.04.0176>, 2015.
- 940 Smolders, E., Baetens, E., Verbeeck, M., Nawara, S., Diels, J., Verdriev, M., Peeters, B., De Cooman, W., and Baken, S.: Internal Loading and Redox Cycling of Sediment Iron Explain Reactive Phosphorus Concentrations in Lowland Rivers, *Environmental Science & Technology*, 51, 2584–2592, <https://doi.org/10.1021/acs.est.6b04337>, 2017.
- Thompson, S.E., Basu, N.B., Lascrain, J., Jr., Aubeneau, A., and Rao, P.S.C.: Relative dominance of hydrologic versus biogeochemical factors on solute export across impact gradients, *Water Resources Research*, 47, <https://doi.org/10.1029/2010wr009605>, 2011.
- 945 Ury, E.A., Arrumugam, P., Herbert, E.R., Badiou, P., Page, B., and Basu, N.B.: Source or sink? Meta-analysis reveals diverging controls of phosphorus retention and release in restored and constructed wetlands, *Environmental Research Letters*, 18, 083002, <https://doi.org/10.1088/1748-9326/ace6bf>, 2023.
- USEPA: National Hydrography Dataset Plus Version 2, U.S. Environmental Protection Agency, Available from: <https://www.epa.gov/waterdata/get-nhdplus-national-hydrography-dataset-plus-data> [Accessed May 23, 2023], 2019.
- 955 USGS: USGS Streamgage NHDPlus Version 1 Basins 2011, U.S. Geological Survey, Available from: <https://water.usgs.gov/GIS/metadata/usgswrd/XML/streamgagebasins.xml#stdorder> [Accessed February 22, 2023], 2012.
- Valayamkunnath, P., Barlage, M., Chen, F., Gochis, D.J., and Franz, K.J.: Mapping of 30-meter resolution tile-drained croplands using a geospatial modeling approach, *Scientific Data* 7, <https://doi.org/10.1038/s41597-020-00596-x>, 2020.
- 960 van Dael, T., De Cooman, T., and Smolders, E.: In-stream oxygenation to mitigate internal loading of phosphorus in lowland streams, *Journal of Hydrology*, 590, 125536, <https://doi.org/10.1016/j.jhydrol.2020.125536>, 2020.
- Vilmin, L., Bouwman, A.F., Beusen, A.H.W., van Hoek, W.J., and Mogollón, J.M.: Past anthropogenic activities offset dissolved inorganic phosphorus retention in the Mississippi River basin, *Biogeochemistry*, 161, 157–169, <https://doi.org/10.1007/s10533-022-00973-1>, 2022.
- 965 Vissers, M.A., Roy, J.W., Yates, A.G., Robinson, K., Rakhimbekova, S., and Robinson, C.E.: Spatio-temporal variability of porewater phosphorus concentrations in streambed sediments of an agricultural stream, *Journal of Hydrology*, 617, 129133, <https://doi.org/10.1016/j.jhydrol.2023.129133>, 2023.
- Wanner, O., Egli, T., Fleischmann, T., Lanz, K., Reichert, P., and Schwarzenbach, R.P.: Behavior of the insecticides disulfoton and thiometon in the Rhine River: a chemodynamic study, *Environmental Science & Technology*, 23, 1232–1242, <https://doi.org/10.1021/es00068a007>, 1989.
- 970 Wright, M.N., and Ziegler, A.: ranger: A Fast Implementation of Random Forests for High Dimensional Data in C++ and R, *Journal of Statistical Software*, 77, <https://doi.org/10.18637/jss.v077.i01>, 2017.

<https://doi.org/10.5194/egusphere-2024-691>

Preprint. Discussion started: 3 May 2024

© Author(s) 2024. CC BY 4.0 License.

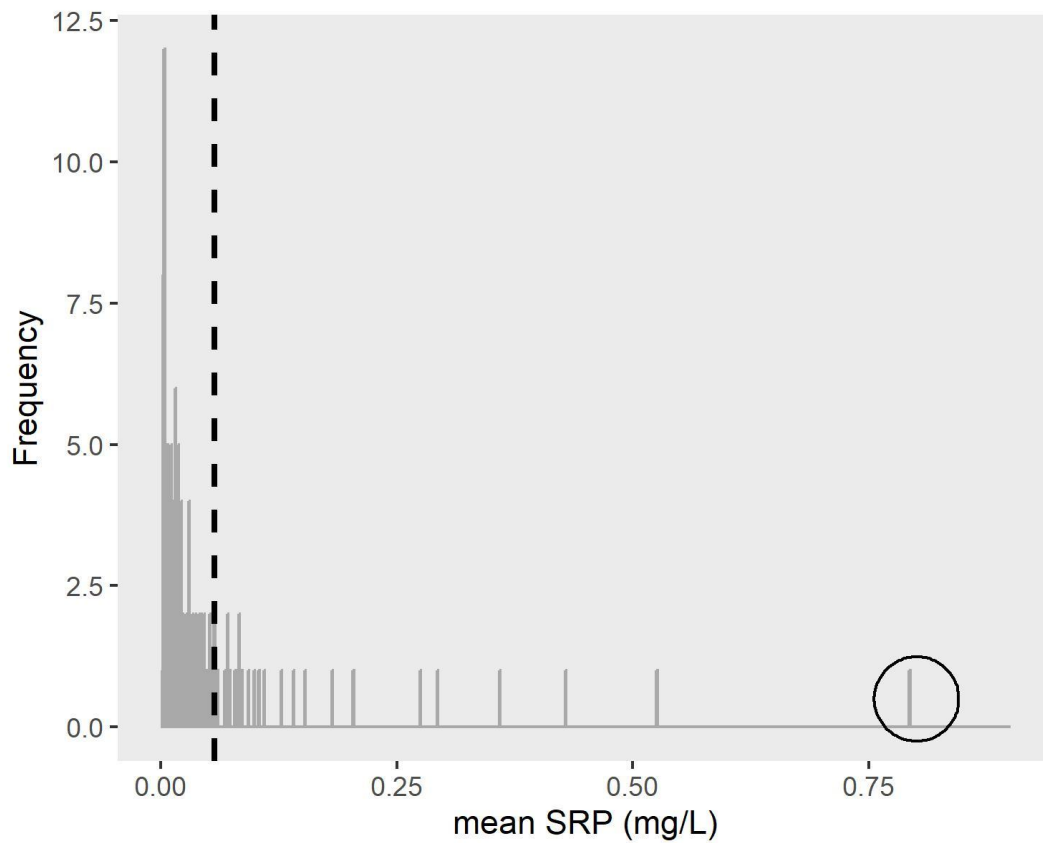


975

Zeng, Q., Qin, L., Bao, L., Li, Y., and Li, X.: Critical nutrient thresholds needed to control eutrophication and synergistic interactions between phosphorus and different nitrogen sources, *Environmental Science and Pollution Research*, 23, 21008–21019, <https://doi.org/10.1007/s11356-016-7321-x>, 2016.



Appendix A



980

Figure A1. Distribution of mean SRP concentrations (mg/L) during late summer low flow conditions for 128 gaged watersheds with ≥ 3 SRP samples collected during late summer low flows. Note that one outlier (circled value) was excluded prior to model development.



985

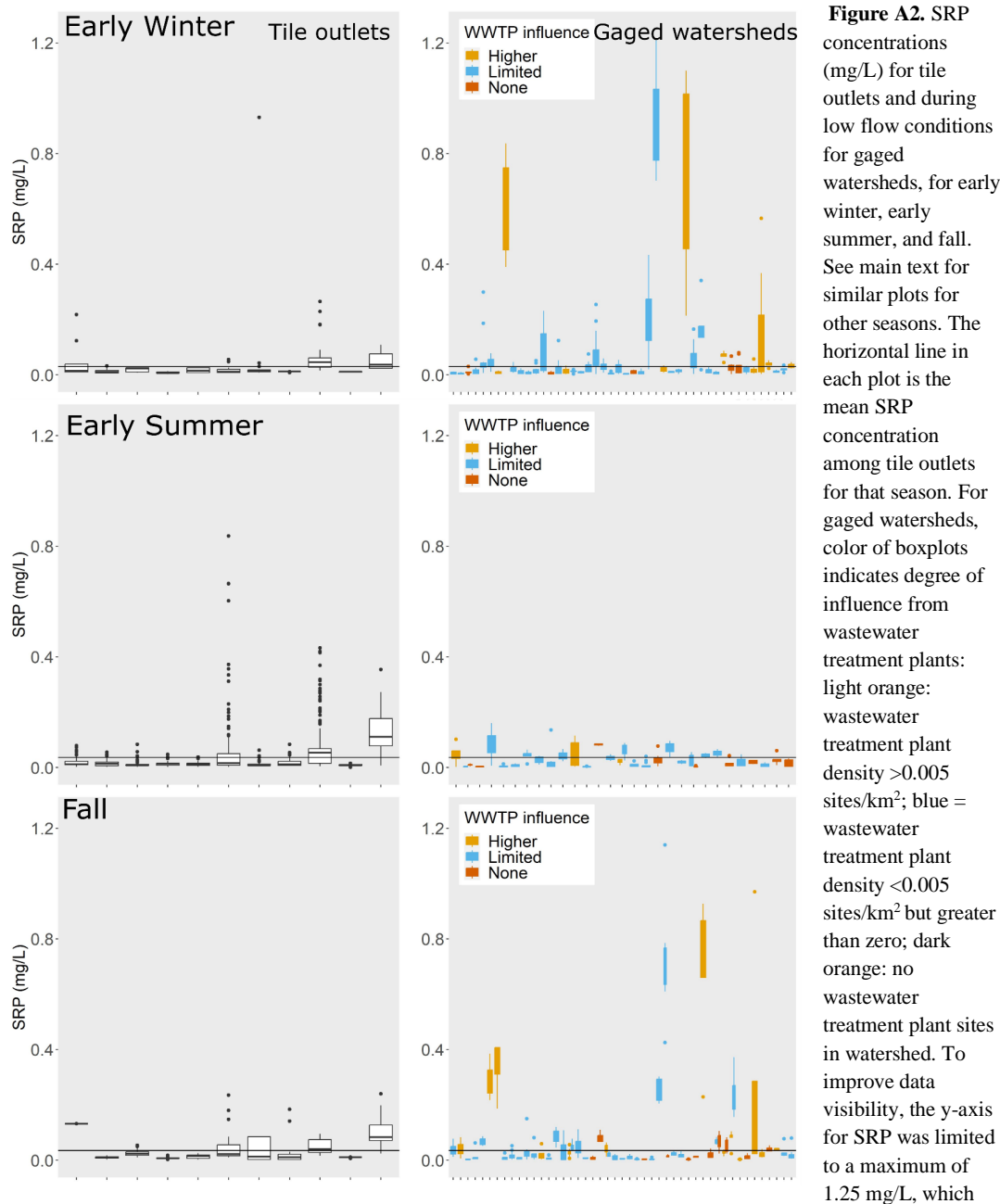
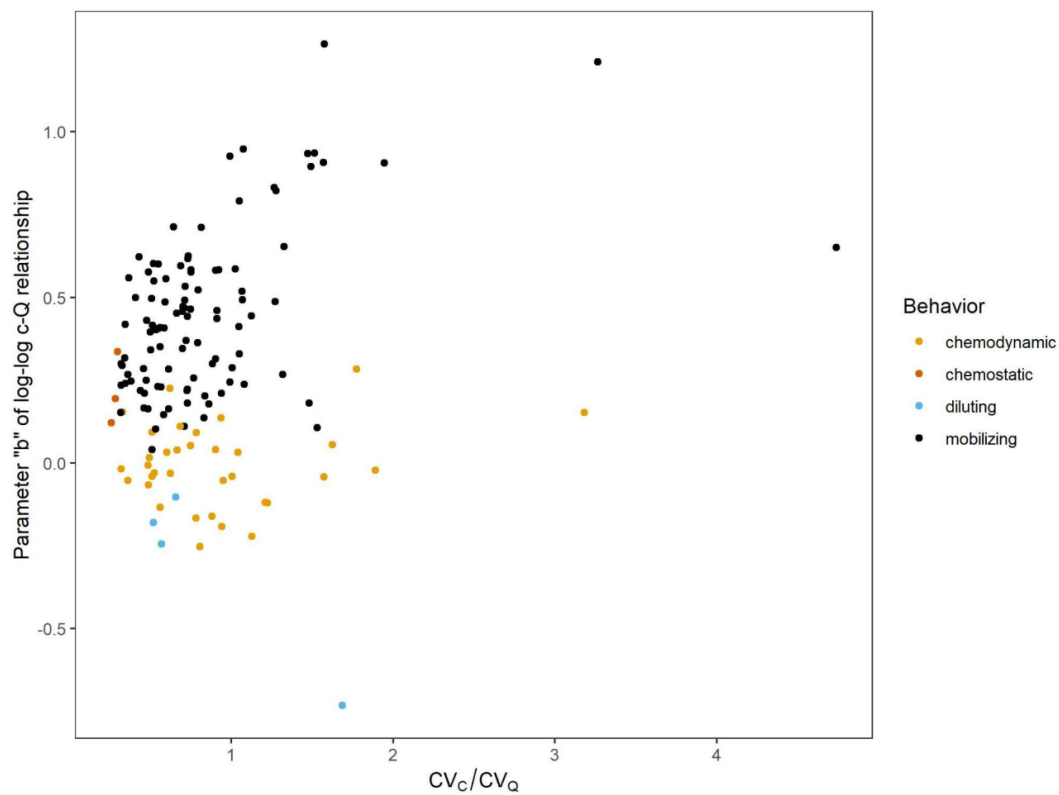


Figure A2. SRP concentrations (mg/L) for tile outlets and during low flow conditions for gaged watersheds, for early winter, early summer, and fall. See main text for similar plots for other seasons. The horizontal line in each plot is the mean SRP concentration among tile outlets for that season. For gaged watersheds, color of boxplots indicates degree of influence from wastewater treatment plants: light orange: wastewater treatment plant density >0.005 sites/km²; blue = wastewater treatment plant density <0.005 sites/km² but greater than zero; dark orange: no wastewater treatment plant sites in watershed. To improve data visibility, the y-axis for SRP was limited to a maximum of 1.25 mg/L, which

1030

eliminated a small number of outliers from the plots for tile outlets (n=34 out of 11,079 records) and gaged watersheds (n=16 out of 2,696 low flow records). Note that not all watersheds had sufficient samples collected during low flows in each season to generate boxplots.



1035 **Figure A3.** Parameter b (slope) of the event-scale log-log C-Q relationship for soluble reactive phosphorus (SRP, mg/L) in relation to CV_c/CV_q for 143 gaged watersheds. Color indicates export behavior based on criteria defined for b and CV_c/CV_q : Chemostatic: $CV_c/CV_q \leq 0.3$ (*sensu* Thompson et al., 2011); chemodynamic: $CV_c/CV_q > 0.3$ and no significant b ($p > 0.05$); diluting: significant $b < 0$; mobilizing: significant $b > 0$.

1040

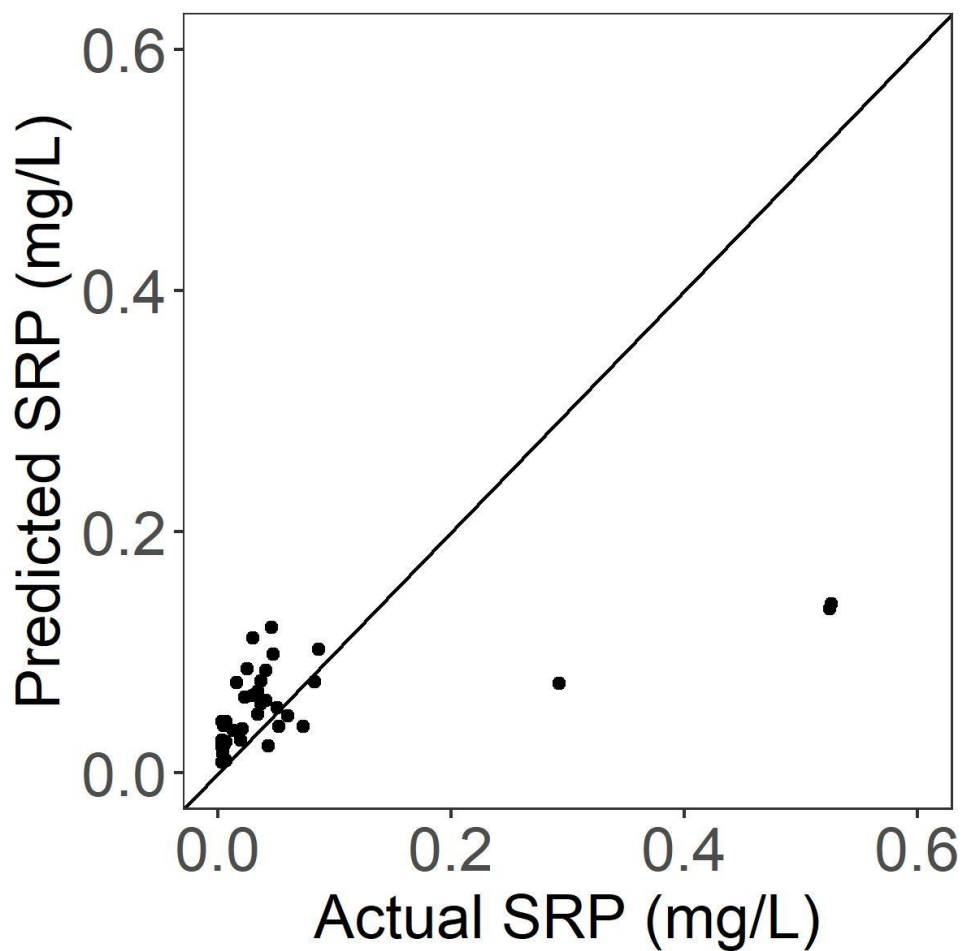


Figure A4. Actual vs predicted late summer SRP concentrations (mg/L) for gaged streams and rivers in the independent test dataset (i.e., not used to build the model). $R^2=0.41$, $RMSE=0.010$, $p < 0.0001$. Solid line shows 1-1 relationship.

1045



Table A1. Linear regression statistics for mean SRP (log scale) during low flow conditions in relation to the density of wastewater treatment plants (sites/km²) across gaged watersheds, by season. Linear regression were calculated with all sites, and recalculated where sites with density of wastewater treatment plants >0.005 sites/km² were excluded.

1050

Season	Slope	T statistic	p	R2	n	WWTP influence
Early Winter	102.77	4.06	<0.001	0.26	50	all watersheds
Early Winter	87.12	1.61	0.12	0.06	40	gages with WWTP >0.005 sites/km ² excluded
Late Winter	90.57	3.62	<0.001	0.19	57	all watersheds
Late Winter	121.36	2.14	0.04	0.1	45	gages with WWTP >0.005 sites/km ² excluded
Spring	29.47	0.7	0.49	0.02	23	all watersheds
Spring	-55.71	-0.7	0.5	0.03	17	gages with WWTP >0.005 sites/km ² excluded
Early Summer	51.93	1.4	0.17	0.05	40	all watersheds
Early Summer	47.84	0.91	0.37	0.02	35	gages with WWTP >0.005 sites/km ² excluded
Late Summer	74.76	4.84	<0.001	0.16	128	all watersheds
Late Summer	80.66	2.44	0.02	0.06	102	gages with WWTP >0.005 sites/km ² excluded
Fall	76.03	4.07	<0.001	0.2	68	all watersheds
Fall	95.19	1.85	0.07	0.07	51	gages with WWTP >0.005 sites/km ² excluded



1055

Table A2. Linear regression statistics for mean SRP (log scale) during low flow conditions in relation to % crop cover across gaged watersheds, by season. Linear regression were calculated with all sites, and recalculated for sites with no wastewater treatment plant influence in their watersheds.

Season	Slope	T statistic	p	R2	n	WWTP influence
Early Winter	0.01	5.09	<0.001	0.35	50	all watersheds
Early Winter	0.01	4.25	0.02	0.86	5	no WWTP present in watershed
Late Winter	0.02	7.65	<0.001	0.52	57	all watersheds
Late Winter	0.01	2.5	0.04	0.44	10	no WWTP present in watershed
Spring	0.01	3.75	<0.001	0.4	23	all watersheds
Spring	0.01	2.27	0.06	0.43	9	no WWTP present in watershed
Early Summer	0.01	3.56	<0.001	0.25	40	all watersheds
Early Summer	0.01	3.32	0.01	0.55	11	no WWTP present in watershed
Late Summer	0.01	10.66	<0.001	0.47	128	all watersheds
Late Summer	0.01	7.39	<0.001	0.69	26	no WWTP present in watershed
Fall	0.01	5.63	<0.001	0.32	68	all watersheds
Fall	0.01	3.09	0.01	0.51	11	no WWTP present in watershed



Table A3. Mean SRP during low flow conditions (flow conditions \leq lowest 25th percentile of flows on record) for each gaged watershed during each season. Note means were only calculated where gaged watersheds had \geq 3 low flow samples collected during a season. Bolded values indicate mean SRP was higher than average tile concentrations during that season. ‘NA’ indicates no data collected during low flow during that season. Shaded values in WWTP density column indicate wastewater treatment plant density was $>$ 0.005 sites/km².

Site name	Human impact	WWTP Density (sites/km ²)	Early Winter	Late Winter	Spring	Early Summer	Late Summer	Fall
Baptism River nr Beaver Bay, MN61	Less Impacted	0.0028	0.006	0.003	NA	NA	0.004	NA
Beaver Creek nr Beaver Falls, CSAH2	Impacted	0.004	NA	NA	NA	NA	0.053	0.041
Beaver River nr Beaver Bay, 1.2mi us of MN61	Impacted	0.0031	NA	NA	NA	NA	0.003	NA
Big Cobb River nr Beauford, CSAH16	Impacted	0.0064	NA	NA	NA	0.048	0.041	0.042
Big Fork River at Big Falls, MN	Less Impacted	8.00E-04	0.005	0.011	NA	0.003	0.004	0.003
Big Fork River nr Bigfork, MN6	Less Impacted	0	NA	NA	NA	0.01	0.007	NA
Big Fork River nr Craigville, MN6	Less Impacted	8.00E-04	NA	NA	NA	NA	0.004	NA
Big Sucker Creek nr Palmers, CR258	Less Impacted	0	0.011	0.009	NA	3.00E-03	0.003	NA
Blue Earth River nr Rapidan, MN	Impacted	0.0043	0.015	0.028	NA	NA	0.015	0.006
Blue Earth River nr Winnebago, CSAH12	Impacted	0.0045	NA	NA	NA	NA	0.027	0.025
Bois de Sioux River nr Doran, MN	Impacted	0.0019	0.069	0.128	NA	0.084	0.086	NA
Boy River nr Boy River, CSAH53	Less Impacted	0.0013	NA	NA	NA	NA	0.002	NA
Brule River nr Hovland, MN61	Less Impacted	0	NA	NA	NA	NA	NA	NA
Buffalo Creek nr Glencoe, CSAH1	Impacted	0.0041	NA	NA	NA	NA	0.793	NA
Buffalo River nr Georgetown, CR108	Impacted	0.0021	0.042	0.052	NA	NA	0.093	0.067



Buffalo River nr Glyndon, CSAH19	Impacted	0.004	NA	NA	NA	NA	0.068	NA
Buffalo River nr Hawley, MN	Impacted	0.0012	NA	NA	NA	NA	0.06	NA
Cannon River at Morristown, CSAH16	Impacted	0.008	NA	NA	0.121	NA	NA	0.29
Cannon River at Welch, MN	Impacted	0.0072	0.009	0.044	NA	NA	0.204	NA
Cedar River nr Austin, MN	Impacted	0.0126	0.65	0.954	NA	NA	0.525	0.338
Chippewa River nr Clontarf, CSAH22	Impacted	0.0035	NA	NA	NA	NA	0.016	0.009
Chippewa River nr Milan, MN40	Impacted	0.0019	2.00E-02	0.027	NA	NA	0.022	0.009
Clearwater River at Plummer, MN	Impacted	0.0021	NA	NA	NA	NA	0.043	0.027
Clearwater River at Red Lake Falls, MN	Impacted	0.002	0.01	0.04	NA	NA	0.009	0.009
Clearwater River nr Clearwater, CR145	Impacted	0.0023	NA	NA	0.008	NA	0.003	NA
Cloquet River nr Brimson, CSAH44	Less Impacted	0	NA	NA	NA	NA	0.004	NA
Cloquet River nr Burnett, CR694	Less Impacted	0.001	0.008	NA	0.005	0.005	0.003	NA
Cottonwood River nr Leavenworth, CR8	Impacted	0.0035	NA	NA	NA	NA	0.013	NA
Cottonwood River nr New Ulm, MN68	Impacted	0.0033	0.016	0.048	0.01	0.007	0.007	0.007
East Branch Blue Earth River at Blue Earth, CSAH16	Impacted	0.0026	NA	NA	NA	NA	0.071	0.062
East Branch Chippewa River nr Benson, CR78	Impacted	8.00E-04	NA	NA	NA	0.043	0.048	0.019
East Fork Rapid River nr Clementson, CSAH18	Less Impacted	0	NA	NA	NA	NA	0.022	NA
Elk River nr Big Lake, MN	Impacted	0.0029	NA	NA	NA	0.027	NA	NA
Hawk Creek nr Granite Falls, CR52	Impacted	0.003	0.083	0.158	NA	0.003	0.01	0.013
Hawk Creek nr Maynard, MN23	Impacted	0.0033	NA	NA	NA	0.056	0.051	0.034
High Island Creek nr Arlington, CR9	Impacted	0	NA	NA	0.037	NA	0.079	NA



High Island Creek nr Henderson, CSAH6	Impacted	0.0016	NA	NA	NA	NA	0.019	NA
Kawishiwi River nr Winton, CSAH18	Less Impacted	0	0.007	0.007	0.004	NA	0.004	NA
Lac qui Parle River nr Lac qui Parle, CSAH31	Impacted	0.0044	0.028	0.063	NA	0.042	0.019	NA
Lac qui Parle River nr Providence, CSAH23	Impacted	0.0041	NA	NA	NA	NA	0.023	NA
Le Sueur River at St. Clair, CSAH28	Impacted	0.0065	NA	NA	0.023	0.101	0.058	NA
Le Sueur River nr Rapidan, CR8	Impacted	0.0052	NA	NA	0.004	0.017	0.029	0.027
Le Sueur River nr Rapidan, MN	Impacted	0.0052	0.014	0.032	NA	0.006	0.014	0.012
Leaf River nr Staples, CSAH29	Impacted	0.0031	0.013	0.025	NA	NA	0.022	NA
Leech Lake River nr Ball Club, CR139	Impacted	0.0014	NA	NA	0.004	0.003	0.004	NA
Little Beauford Ditch nr Beauford, MN22	Impacted	0	NA	NA	0.025	0.083	0.153	NA
Little Fork River at Little Fork, MN	Less Impacted	5.00E-04	0.009	0.015	NA	NA	0.004	0.004
Little Fork River nr Linden Grove, TH73	Impacted	0.0027	NA	NA	NA	NA	0.02	0.018
Little Fork River nr Littlefork, MN65	Less Impacted	6.00E-04	NA	NA	NA	NA	0.007	0.005
Long Prairie River at Long Prairie, MN	Impacted	0.0055	NA	0.016	0.014	NA	NA	NA
Long Prairie River at Philbrook, 313th Ave	Impacted	0.0047	0.024	0.022	NA	0.035	0.023	NA
Lost River nr Brooks, CR119	Impacted	0.0026	NA	NA	NA	NA	0.042	0.085
Maple River nr Rapidan, CR35	Impacted	0.0046	NA	NA	NA	NA	0.02	0.038
Maple River nr Sterling Center, CR18	Impacted	0.0037	NA	NA	NA	NA	0.071	NA
Middle Branch Root River nr Fillmore, CSAH5	Impacted	0.0059	NA	NA	NA	NA	0.039	0.035
Middle Fork Crow River nr Manannah, CSAH30	Impacted	0.0057	NA	NA	0.01	0.022	0.012	NA
Middle Fork Zumbro River nr Oronoco, 5th St	Impacted	0.0056	NA	NA	NA	NA	0.041	0.02



Middle River at Argyle, MN	Impacted	0.0016	NA	NA	NA	0.062	0.043	0.048
Minnesota River at Judson, CSAH42	Impacted	0.0031	0.04	0.08	NA	1.00E-02	0.027	0.028
Minnesota River at Morton, MN	Impacted	0.003	0.098	0.141	NA	NA	0.046	0.058
Minnesota River nr Lac qui Parle, MN	Impacted	0.0033	0.094	0.126	NA	NA	0.085	0.055
Mississippi River at Grand Rapids, MN	Impacted	0.0014	NA	0.003	0.003	0.003	0.005	0.007
Mississippi River nr Bemidji, CSAH11	Impacted	0.001	NA	NA	NA	0.028	0.03	NA
Mississippi River nr Bemidji, MN	Impacted	0.0025	NA	NA	NA	0.003	0.003	NA
Mud River nr Grygla, MN89	Impacted	0	NA	NA	NA	0.029	0.021	0.008
Mustinka River nr Norcross, MN9	Impacted	0	NA	NA	NA	NA	0.083	0.082
Nemadji River nr Pleasant Valley, MN23	Impacted	0	NA	NA	NA	NA	0.005	NA
North Fork Crow River nr Cokato, CSAH4	Impacted	0.0042	NA	NA	NA	0.07	0.031	NA
North Fork Crow River nr Rockford, Farmington Ave	Impacted	0.0046	0.031	0.045	NA	NA	0.02	0.021
North Fork Whitewater River at Elba, Whitewater Dr	Impacted	0.0111	NA	0.049	NA	NA	NA	0.057
North Fork Zumbro River nr Mazeppa, CSAH7	Impacted	0.0064	NA	0.046	NA	NA	0.057	0.026
Otter Tail River at Breckenridge, CSAH16	Impacted	0.0018	0.005	0.01	NA	NA	0.016	0.011
Otter Tail River nr Elizabeth, MN	Impacted	0.0013	NA	0.005	NA	NA	0.003	0.002
Pelican River nr Fergus Falls, MN210	Impacted	0.0031	NA	NA	NA	2.00E-02	0.019	0.006
Pine River nr Jenkins, CSAH15	Impacted	0	NA	NA	NA	NA	NA	NA
Pipestone Creek nr Pipestone, CSAH13	Impacted	0.0065	NA	NA	NA	NA	0.025	NA
Pomme De Terre River at Appleton, MN	Impacted	0.0022	0.024	0.082	NA	NA	NA	NA



Pomme de Terre River nr Hoffman, CR76	Impacted	0.0019	NA	NA	NA	NA	0.013	0.01
Poplar River nr Lutsen, 0.2mi US of MN61	Less Impacted	0.0034	0.004	0.003	NA	NA	0.003	0.003
Prairie River nr Taconite, MN	Impacted	0	NA	0.006	0.006	NA	0.005	NA
Rapid River at Clementson, MN11	Impacted	0	0.01	0.014	NA	NA	0.004	0.003
Red Lake River at Fisher, MN	Impacted	0.001	0.009	0.017	NA	0.034	0.013	NA
Red Lake River at High Landing nr Goodridge, MN	Impacted	0	NA	NA	NA	0.003	0.011	NA
Red Lake River at Red Lake Falls, CR13	Impacted	4.00E-04	NA	NA	0.003	0.023	0.004	0.004
Red River of the North nr Kragnes, CSAH26	Impacted	0.0027	0.217	0.332	NA	NA	0.275	0.254
Redwood River at Russell, CR15	Impacted	0	NA	NA	NA	NA	0.035	0.015
Redwood River nr Redwood Falls, MN	Impacted	0.0031	1.18E+00	1.247	NA	NA	0.099	0.731
Rock River at Luverne, CR4	Impacted	0.0055	0.02	0.025	NA	NA	0.016	NA
Rum River at Anoka, headwater side of dam	Impacted	0.0044	0.01	0.015	NA	0.043	NA	NA
S Br. Wild Rice River at CR27 nr Felton, MN	Impacted	0.006	NA	NA	NA	NA	0.055	NA
Sand Hill River at Climax, MN, US-75	Impacted	8.00E-04	0.014	0.031	NA	NA	0.034	0.024
Sandhill River nr Fertile, 450th St SW	Impacted	0.0016	NA	NA	NA	0.052	0.029	0.018
Sauk River nr St. Martin, CR12	Impacted	0.0048	NA	NA	0.018	NA	0.059	NA
Second Creek nr Aurora, 0.6mi us of CSAH110	Impacted	0	NA	0.006	NA	NA	0.004	0.002
Seven Mile Creek nr St. Peter, 0.6mi us of US169	Impacted	0	NA	0.027	0.008	0.015	0.016	0.012
Shakopee Creek nr Benson, 20th Ave SW	Impacted	0	NA	0.024	0.006	NA	0.141	NA
Shell Rock River nr Gordonsville, CSAH1	Impacted	0.0121	1.159	1.368	NA	NA	0.526	0.68



Sleepy Eye Creek nr Cobden, CR8	Impacted	0	NA	NA	NA	NA	0.022	0.021
Snake River above Warren, MN	Impacted	0	NA	NA	NA	NA	NA	0.068
Snake River nr Big Woods, MN220	Impacted	0.001	0.074	0.191	NA	NA	NA	0.068
Snake River nr Pine City, MN	Impacted	0.0027	0.014	0.02	NA	0.02	0.012	NA
South Branch Buffalo River nr Glyndon, 28th Ave S	Impacted	8.00E-04	NA	NA	NA	NA	0.128	NA
South Branch Middle Fork Zumbro River nr Oronoco, 5th St	Impacted	0.0105	NA	NA	NA	NA	0.057	0.025
South Branch Root River at Lanesboro, Rochelle Ave N	Impacted	0.0095	NA	NA	NA	NA	0.03	0.032
South Branch Two Rivers at Hallock, MN175	Impacted	6.00E-04	NA	NA	NA	NA	0.052	NA
South Branch Two Rivers at Lake Bronson, MN	Impacted	0	NA	NA	NA	NA	0.104	0.053
South Fork Crow River at Delano, Bridge Ave	Impacted	0.0042	0.168	0.218	NA	NA	0.182	0.239
South Fork Watonwan River nr Madelia, CSAH13	Impacted	0.0039	NA	NA	NA	NA	0.052	NA
South Fork Zumbro River nr Oronoco, CR121	Impacted	0.0147	NA	NA	NA	NA	0.11	0.077
Split Rock Creek nr Jasper, 201st St	Impacted	0.0036	1.40E-02	0.027	NA	NA	0.011	NA
Spring Creek nr Hanley Falls, 480th St	Impacted	0.006	NA	NA	NA	NA	0.293	NA
St. Francis River nr Big Lake, 164th St	Impacted	0	NA	NA	NA	0.02	0.013	NA
St. Louis River at Floodwood, CSAH8	Impacted	0.0042	NA	NA	0.002	NA	0.011	NA
St. Louis River at Scanlon, MN	Impacted	0.0034	0.007	NA	NA	0.009	0.004	NA
St. Louis River nr Forbes, US53	Impacted	0.0056	NA	NA	0.003	NA	0.004	0.003
Stony River nr Babbitt, Tomahawk Rd	Less Impacted	0	NA	NA	NA	NA	0.003	NA
Straight River nr Faribault, MN	Impacted	0.0062	0.069	NA	NA	NA	NA	NA



Sunrise River at Sunrise, CR88	Impacted	0.0046	NA	NA	NA	NA	0.037	NA
Swan River nr Jacobson, CR438	Impacted	0.0119	NA	NA	NA	NA	0.018	NA
Swan River nr Sobieski, MN238	Impacted	0.0022	NA	NA	NA	NA	0.021	NA
Tamarac River nr Florian, CSAH1	Impacted	0	NA	NA	NA	0.022	0.011	NA
Tamarac River nr Stephen, CSAH22	Impacted	0	0.03	0.198	NA	3.60E-02	NA	NA
Thief River downstream of CSAH 7, 6 mi E of Holt	Impacted	0	NA	0.036	0.002	0.013	0.007	NA
Thief River nr Thief River Falls, MN	Impacted	0	0.026	0.05	NA	0.027	0.011	0.012
Turtle Creek at Austin, 43rd St	Impacted	0.0078	NA	NA	NA	NA	0.359	0.268
Twelvemile Creek nr Wheaton, CSAH14	Impacted	0	NA	NA	0.141	NA	0.429	NA
Two Rivers nr Bowlus, 40th St	Impacted	0.0078	NA	NA	NA	NA	NA	NA
Two Rivers nr Hallock, CSAH16	Impacted	4.00E-04	0.018	0.03	NA	NA	0.016	NA
Watonwan River nr Garden City, CSAH13	Impacted	0.005	0.017	0.152	NA	NA	0.016	0.022
Watonwan River nr La Salle, CSAH3	Impacted	0.0046	NA	NA	NA	NA	0.073	NA
Wells Creek nr Frontenac, US61	Impacted	0	NA	NA	0.032	NA	NA	0.04
West Branch Lac qui Parle River at Dawson, Diagonal St	Impacted	0.0025	NA	NA	NA	NA	0.083	NA
West Branch Rum River nr Princeton, CR102	Impacted	0.0062	NA	NA	NA	NA	NA	NA
West Fork Des Moines River at Jackson, River St	Impacted	0.0068	0.342	0.592	NA	NA	0.037	NA
West Fork Des Moines River nr Avoca, CSAH6	Impacted	0.0065	NA	NA	NA	NA	0.014	NA
Whitewater River nr Beaver, CSAH30	Impacted	0.0102	0.039	0.048	NA	NA	0.047	0.039
Wild Rice River at Hendrum, MN	Impacted	0.002	0.012	0.018	NA	NA	0.03	0.031
Wild Rice River at Twin Valley, MN	Impacted	0.0012	NA	NA	NA	NA	0.007	NA



Wild Rice River nr Mahnomon, CSAH25	Impacted	0	NA	NA	NA	NA	0.019	NA
Yellow Bank River nr Odessa, CSAH40	Impacted	0.0042	0.021	0.31	NA	NA	0.03	NA
Yellow Medicine River nr Granite Falls, MN	Impacted	0.0023	0.02	0.35	NA	NA	0.034	0.012
Yellow Medicine River nr Hanley Falls, CR18	Impacted	9.00E-04	NA	NA	NA	NA	0.019	0.027
Zumbro River at Kellogg, US61	Impacted	0.0084	0.033	0.042	NA	NA	0.046	NA



Table A4. Number of SRP samples collected during low flow conditions in each season for each gaged watershed. Note that mean SRP values (Table S3) were only calculated in seasons where ≥ 3 samples had been collected during low flow conditions for that gaged watershed.

Site name	Early Winter	Late Winter	Spring	Early Summer	Late Summer	Fall
Baptism River nr Beaver Bay, MN61	4	5	NA	2	9	NA
Beaver Creek nr Beaver Falls, CSAH2	NA	1	1	1	6	5
Beaver River nr Beaver Bay, 1.2mi us of MN61	NA	NA	NA	2	4	1
Big Cobb River nr Beauford, CSAH16	NA	2	2	4	18	4
Big Fork River at Big Falls, MN	6	10	1	4	14	3
Big Fork River nr Bigfork, MN6	NA	NA	NA	4	14	NA
Big Fork River nr Craigville, MN6	NA	NA	NA	2	10	1
Big Sucker Creek nr Palmers, CR258	6	4	NA	3	4	NA
Blue Earth River nr Rapidan, MN	11	7	2	2	19	3
Blue Earth River nr Winnebago, CSAH12	NA	1	NA	NA	8	3
Bois de Sioux River nr Doran, MN	10	5	2	6	12	2
Boy River nr Boy River, CSAH53	NA	NA	1	2	5	2
Brule River nr Hovland, MN61	NA	NA	NA	NA	1	2
Buffalo Creek nr Glencoe, CSAH1	NA	1	2	1	3	1
Buffalo River nr Georgetown, CR108	8	7	NA	NA	11	4
Buffalo River nr Glyndon, CSAH19	NA	NA	NA	NA	3	2
Buffalo River nr Hawley, MN	NA	2	1	NA	4	2
Cannon River at Morrystown, CSAH16	NA	1	3	NA	2	3
Cannon River at Welch, MN	8	5	1	NA	6	1
Cedar River nr Austin, MN	10	4	NA	1	9	4
Chippewa River nr Clontarf, CSAH22	NA	2	1	2	5	4
Chippewa River nr Milan, MN40	11	8	NA	NA	9	4
Clearwater River at Plummer, MN	NA	NA	2	NA	5	6



Clearwater River at Red Lake Falls, MN	14	9	2	1	16	9
Clearwater River nr Clearwater, CR145	NA	2	3	1	3	1
Cloquet River nr Brimson, CSAH44	NA	NA	1	1	7	NA
Cloquet River nr Burnett, CR694	3	2	4	4	13	2
Cottonwood River nr Leavenworth, CR8	NA	NA	2	1	6	2
Cottonwood River nr New Ulm, MN68	14	8	3	3	14	6
East Branch Blue Earth River at Blue Earth, CSAH16	NA	1	NA	1	8	3
East Branch Chippewa River nr Benson, CR78	NA	NA	NA	6	6	3
East Fork Rapid River nr Clementson, CSAH18	NA	NA	1	2	8	NA
Elk River nr Big Lake, MN	NA	1	2	5	2	1
Hawk Creek nr Granite Falls, CR52	13	7	1	3	12	5
Hawk Creek nr Maynard, MN23	NA	1	2	3	5	4
High Island Creek nr Arlington, CR9	NA	1	4	1	5	1
High Island Creek nr Henderson, CSAH6	NA	1	2	1	8	1
Kawishiwi River nr Winton, CSAH18	3	6	3	1	5	1
Lac qui Parle River nr Lac qui Parle, CSAH31	9	4	2	3	5	2
Lac qui Parle River nr Providence, CSAH23	NA	NA	NA	NA	3	2
Le Sueur River at St. Clair, CSAH28	NA	1	3	4	14	2
Le Sueur River nr Rapidan, CR8	NA	2	3	6	17	4
Le Sueur River nr Rapidan, MN	16	7	1	3	19	4
Leaf River nr Staples, CSAH29	7	9	NA	1	7	NA
Leech Lake River nr Ball Club, CR139	1	2	3	5	8	1



Little Beauford Ditch nr Beauford, MN22	NA	NA	8	3	14	2
Little Fork River at Little Fork, MN	7	9	NA	1	11	4
Little Fork River nr Linden Grove, TH73	NA	NA	NA	NA	4	3
Little Fork River nr Littlefork, MN65	NA	NA	NA	1	8	6
Long Prairie River at Long Prairie, MN	NA	3	4	1	1	2
Long Prairie River at Philbrook, 313th Ave	14	11	1	3	5	2
Lost River nr Brooks, CR119	NA	NA	NA	NA	12	3
Maple River nr Rapidan, CR35	NA	NA	NA	2	11	3
Maple River nr Sterling Center, CR18	NA	1	NA	2	15	2
Middle Branch Root River nr Fillmore, CSAH5	NA	NA	NA	NA	8	5
Middle Fork Crow River nr Manannah, CSAH30	NA	1	3	3	3	2
Middle Fork Zumbro River nr Oronoco, 5th St	NA	1	NA	NA	8	5
Middle River at Argyle, MN	NA	NA	NA	3	3	4
Minnesota River at Judson, CSAH42	12	6	NA	4	14	5
Minnesota River at Morton, MN	12	5	NA	1	7	8
Minnesota River nr Lac qui Parle, MN	5	5	NA	2	3	4
Mississippi River at Grand Rapids, MN	2	5	8	8	13	4
Mississippi River nr Bemidji, CSAH11	NA	NA	NA	3	3	1
Mississippi River nr Bemidji, MN	NA	NA	1	3	4	1
Mud River nr Grygla, MN89	NA	NA	NA	8	15	3
Mustinka River nr Norcross, MN9	NA	NA	2	1	6	3
Nemadji River nr Pleasant Valley, MN23	NA	NA	NA	1	6	1



North Fork Crow River nr Cokato, CSAH4	NA	1	2	3	3	1
North Fork Crow River nr Rockford, Farmington Ave	5	7	NA	2	4	3
North Fork Whitewater River at Elba, Whitewater Dr	NA	3	2	1	2	3
North Fork Zumbro River nr Mazeppa, CSAH7	NA	3	2	NA	4	4
Otter Tail River at Breckenridge, CSAH16	10	7	NA	1	11	8
Otter Tail River nr Elizabeth, MN	NA	7	1	1	7	3
Pelican River nr Fergus Falls, MN210	NA	NA	2	4	5	3
Pine River nr Jenkins, CSAH15	NA	NA	NA	1	2	NA
Pipestone Creek nr Pipestone, CSAH13	NA	1	1	1	7	NA
Pomme De Terre River at Appleton, MN	9	7	NA	1	2	2
Pomme de Terre River nr Hoffman, CR76	NA	NA	NA	2	7	3
Poplar River nr Lutsen, 0.2mi US of MN61	3	7	1	1	7	4
Prairie River nr Taconite, MN	NA	3	3	NA	6	2
Rapid River at Clementson, MN11	8	11	1	2	13	3
Red Lake River at Fisher, MN	13	8	NA	4	17	2
Red Lake River at High Landing nr Goodridge, MN	NA	NA	2	4	6	2
Red Lake River at Red Lake Falls, CR13	NA	NA	3	4	8	5
Red River of the North nr Kragnes, CSAH26	14	8	NA	NA	7	4
Redwood River at Russell, CR15	NA	1	2	NA	7	4
Redwood River nr Redwood Falls, MN	12	7	2	1	11	6
Rock River at Luverne, CR4	7	6	1	1	4	2



Rum River at Anoka, headwater side of dam	10	14	1	6	1	NA
S Br. Wild Rice River at CR27 nr Felton, MN	NA	NA	NA	NA	4	1
Sand Hill River at Climax, MN, US-75	10	11	2	1	9	3
Sandhill River nr Fertile, 450th St SW	NA	NA	NA	3	10	4
Sauk River nr St. Martin, CR12	NA	NA	3	2	4	1
Second Creek nr Aurora, 0.6mi us of CSAH110	NA	3	2	1	9	4
Seven Mile Creek nr St. Peter, 0.6mi us of US169	NA	3	9	8	22	5
Shakopee Creek nr Benson, 20th Ave SW	NA	3	4	2	5	2
Shell Rock River nr Gordonsville, CSAH1	9	6	NA	NA	3	5
Sleepy Eye Creek nr Cobden, CR8	NA	NA	1	NA	8	3
Snake River above Warren, MN	NA	NA	2	1	1	3
Snake River nr Big Woods, MN220	13	3	NA	1	2	3
Snake River nr Pine City, MN	4	8	NA	5	7	NA
South Branch Buffalo River nr Glyndon, 28th Ave S	NA	NA	NA	1	7	2
South Branch Middle Fork Zumbro River nr Oronoco, 5th St	NA	1	NA	NA	3	5
South Branch Root River at Lanesboro, Rochelle Ave N	NA	2	NA	1	7	4
South Branch Two Rivers at Hallock, MN175	NA	1	NA	1	4	2
South Branch Two Rivers at Lake Bronson, MN	NA	1	NA	2	3	4
South Fork Crow River at Delano, Bridge Ave	5	7	1	NA	6	4
South Fork Watonwan River nr Madelia, CSAH13	NA	1	NA	NA	6	1
South Fork Zumbro River nr Oronoco, CR121	NA	1	NA	NA	6	5



Split Rock Creek nr Jasper, 201st St	6	7	NA	NA	6	2
Spring Creek nr Hanley Falls, 480th St	NA	1	2	1	7	2
St. Francis River nr Big Lake, 164th St	NA	1	NA	6	5	1
St. Louis River at Floodwood, CSAH8	NA	NA	3	2	5	1
St. Louis River at Scanlon, MN	3	1	1	4	11	2
St. Louis River nr Forbes, US53	NA	NA	3	1	9	5
Stony River nr Babbitt, Tomahawk Rd	NA	1	2	1	6	1
Straight River nr Faribault, MN	5	2	NA	NA	2	NA
Sunrise River at Sunrise, CR88	2	2	NA	NA	4	NA
Swan River nr Jacobson, CR438	NA	NA	2	2	4	1
Swan River nr Sobieski, MN238	NA	NA	NA	NA	3	2
Tamarac River nr Florian, CSAH1	NA	NA	1	4	10	2
Tamarac River nr Stephen, CSAH22	11	6	NA	3	2	NA
Thief River downstream of CSAH 7, 6 mi E of Holt	NA	3	4	5	6	1
Thief River nr Thief River Falls, MN	12	12	1	3	11	3
Turtle Creek at Austin, 43rd St	NA	NA	NA	1	9	4
Twelvemile Creek nr Wheaton, CSAH14	NA	2	3	1	5	1
Two Rivers nr Bowlus, 40th St	NA	NA	NA	2	NA	NA
Two Rivers nr Hallock, CSAH16	11	9	NA	2	9	2
Watonwan River nr Garden City, CSAH13	11	8	1	1	15	3
Watonwan River nr La Salle, CSAH3	NA	1	1	NA	6	2
Wells Creek nr Frontenac, US61	NA	NA	4	1	2	3
West Branch Lac qui Parle River at Dawson, Diagonal St	NA	NA	NA	NA	4	2
West Branch Rum River nr Princeton, CR102	NA	NA	NA	NA	NA	1
West Fork Des Moines River at Jackson, River St	8	8	1	NA	5	2



West Fork Des Moines River nr Avoca, CSAH6	NA	NA	1	1	5	1
Whitewater River nr Beaver, CSAH30	7	5	2	1	5	3
Wild Rice River at Hendrum, MN	8	11	2	1	14	5
Wild Rice River at Twin Valley, MN	NA	1	NA	NA	4	1
Wild Rice River nr Mahnomon, CSAH25	NA	NA	NA	NA	5	NA
Yellow Bank River nr Odessa, CSAH40	6	5	NA	NA	4	2
Yellow Medicine River nr Granite Falls, MN	7	5	2	NA	8	7
Yellow Medicine River nr Hanley Falls, CR18	NA	1	2	NA	7	5
Zumbro River at Kellogg, US61	7	6	NA	NA	9	2
Total number of sites with >=3 samples collected during low flows	50	57	23	40	128	68

Table A5. Linear regression statistics for the log-log relationship between SRP concentrations (mg/L) and normalized flow (Q/Q_{GM}). The regressions were run twice. The first regressions (denoted with (1) in the table) included all samples collected for a given site. The second set of regressions (denoted with (2) in the table) excluded samples collected during late summer low flows. ‘% change in slope’ indicates the change in slope between the first and second regression for each site. CV_c/CV_Q is reported using all samples collected for each site. Statistics in bold indicate statistically significant ($p < 0.05$) relationships.

Site name	Behavior	CV_c/CV_Q	Slope(1)	p(1)	$R^2(1)$	n(1)	Slope(2)	p(2)	$R^2(2)$	n(2)	% slope change
Baptism River nr Beaver Bay, MN61	chemodynamic	0.66	0.04	0.21	0.01	184	0.05	0.14	0.01	175	30.8
Beaver Creek nr Beaver Falls, CSAH2	mobilizing	0.34	0.42	<0.01	0.36	113	0.45	<0.01	0.37	107	7.7
Beaver River nr Beaver Bay, 1.2mi us of MN61	chemodynamic	0.51	0.09	0.20	0.04	48	0.07	0.42	0.02	44	-24.03
Big Cobb River nr Beauford, CSAH16	mobilizing	0.56	0.35	<0.01	0.20	243	0.47	<0.01	0.20	225	32.66
Big Fork River at Big Falls, MN	mobilizing	0.61	0.16	<0.01	0.06	264	0.12	0.01	0.03	250	-26.35



Big Fork River nr Bigfork, MN6	chemodynamic	1.01	-0.04	0.62	0.00	116	-0.01	0.91	0.00	102	-70.13
Big Fork River nr Craigville, MN6	mobilizing	0.73	0.22	<0.01	0.07	112	0.15	0.10	0.03	102	-32.38
Big Sucker Creek nr Palmers, CR258	chemodynamic	0.6	0.03	0.40	0.00	162	0.01	0.71	0.00	158	-54.47
Blue Earth River nr Rapidan, MN	mobilizing	0.74	0.62	<0.01	0.45	437	0.64	<0.01	0.41	418	1.69
Blue Earth River nr Winnebago, CSAH12	mobilizing	0.71	0.47	<0.01	0.27	139	0.50	<0.01	0.22	131	6.3
Bois de Sioux River nr Doran, MN	mobilizing	0.32	0.23	<0.01	0.26	426	0.24	<0.01	0.25	414	2.88
Boy River nr Boy River, CSAH53	chemodynamic	1.77	0.28	0.09	0.06	49	0.29	0.14	0.05	44	0.7
Brule River nr Hovland, MN61	chemodynamic	0.94	0.14	0.17	0.10	21	0.14	0.20	0.09	20	2.09
Buffalo Creek nr Glencoe, CSAH1	chemodynamic	0.95	-0.05	0.56	0.00	71	0.09	0.39	0.01	68	260.73
Buffalo River nr Georgetown, CR108	mobilizing	0.32	0.30	<0.01	0.25	438	0.32	<0.01	0.26	427	7.98
Buffalo River nr Glyndon, CSAH19	mobilizing	0.50	0.40	<0.01	0.28	73	0.46	<0.01	0.32	70	15.25
Buffalo River nr Hawley, MN	mobilizing	0.53	0.40	<0.01	0.27	97	0.43	<0.01	0.28	93	6.76
Cannon River at Morristown, CSAH16	chemodynamic	0.81	-0.25	0.07	0.06	58	-0.20	0.18	0.03	56	-20.19
Cannon River at Welch, MN	mobilizing	1.07	0.49	<0.01	0.09	119	0.68	<0.01	0.17	113	37.33
Cedar River nr Austin, MN	diluting	0.57	-0.25	<0.01	0.19	265	-0.22	<0.01	0.14	256	-12.34
Chippewa River nr Clontarf, CSAH22	mobilizing	1.51	0.94	<0.01	0.28	123	1.03	<0.01	0.29	118	10.1
Chippewa River nr Milan, MN40	mobilizing	1.33	0.65	<0.01	0.29	304	0.68	<0.01	0.28	295	4.66
Clearwater River at Plummer, MN	mobilizing	0.73	0.44	<0.01	0.15	99	0.55	<0.01	0.19	94	24.76



Clearwater River at Red Lake Falls, MN	mobilizing	0.55	0.41	<0.01	0.18	396	0.37	<0.01	0.14	380	-10.15
Clearwater River nr Clearwater, CR145	chemodynamic	1.22	-0.12	0.44	0.01	59	-0.28	0.10	0.05	56	137.88
Cloquet River nr Brimson, CSAH44	chemodynamic	0.62	-0.03	0.75	0.00	80	-0.13	0.29	0.02	73	325.35
Cloquet River nr Burnett, CR694	chemodynamic	1.04	0.03	0.59	0.00	142	-0.02	0.77	0.00	129	165.87
Cottonwood River nr Leavenworth, CR8	mobilizing	0.91	0.46	<0.01	0.35	136	0.47	<0.01	0.27	130	1.75
Cottonwood River nr New Ulm, MN68	mobilizing	0.73	0.62	<0.01	0.49	389	0.60	<0.01	0.44	375	-3.08
East Branch Blue Earth River at Blue Earth, CSAH16	mobilizing	0.84	0.20	<0.01	0.06	140	0.29	<0.01	0.08	132	41.42
East Branch Chippewa River nr Benson, CR78	mobilizing	0.91	0.44	<0.01	0.13	119	0.69	<0.01	0.24	113	57.36
East Fork Rapid River nr Clementson, CSAH18	diluting	0.52	-0.18	<0.01	0.18	93	-0.14	0.01	0.07	85	-24.78
Elk River nr Big Lake, MN	mobilizing	1.12	0.44	0.02	0.09	63	0.50	0.01	0.11	61	11.55
Hawk Creek nr Granite Falls, CR52	mobilizing	0.51	0.50	<0.01	0.37	375	0.44	<0.01	0.31	363	-11.18
Hawk Creek nr Maynard, MN23	chemostatic	0.3	0.34	<0.01	0.30	120	0.34	<0.01	0.29	115	2.35
High Island Creek nr Arlington, CR9	chemodynamic	0.78	0.09	0.12	0.02	100	0.14	0.07	0.03	95	54.04
High Island Creek nr Henderson, CSAH6	mobilizing	0.79	0.36	<0.01	0.20	96	0.33	<0.01	0.11	88	-10.11
Kawishiwi River nr Winton, CSAH18	chemodynamic	1.21	-0.12	0.08	0.02	143	-0.16	0.02	0.04	138	34.45
Lac qui Parle River nr Lac qui Parle, CSAH31	mobilizing	0.71	0.49	<0.01	0.33	186	0.49	<0.01	0.31	181	0.31
Lac qui Parle River nr Providence, CSAH23	mobilizing	0.49	0.58	<0.01	0.40	72	0.70	<0.01	0.44	69	20.68
Le Sueur River at St. Clair, CSAH28	mobilizing	0.34	0.32	<0.01	0.21	179	0.38	<0.01	0.20	165	21.25



Le Sueur River nr Rapidan, CR8	mobilizing	0.43	0.62	<0.01	0.50	269	0.67	<0.01	0.45	252	7.11
Le Sueur River nr Rapidan, MN	mobilizing	0.59	0.56	<0.01	0.46	478	0.55	<0.01	0.42	459	-0.76
Leaf River nr Staples, CSAH29	mobilizing	0.54	0.23	<0.01	0.15	181	0.23	<0.01	0.14	174	-0.59
Leech Lake River nr Ball Club, CR139	chemodynamic	1.63	0.05	0.68	0.00	77	0.05	0.76	0.00	69	-13.76
Little Beauford Ditch nr Beauford, MN22	mobilizing	0.36	0.27	<0.01	0.18	198	0.42	<0.01	0.32	184	57.82
Little Fork River at Little Fork, MN	chemodynamic	0.49	0.02	0.62	0.00	251	-0.04	0.27	0.01	240	336.91
Little Fork River nr Linden Grove, TH73	chemodynamic	0.36	-0.05	0.35	0.02	50	-0.02	0.79	0.00	46	-65.46
Little Fork River nr Littlefork, MN65	chemodynamic	0.49	-0.01	0.88	0.00	113	-0.05	0.36	0.01	105	598.71
Long Prairie River at Long Prairie, MN	mobilizing	1.05	0.41	<0.01	0.14	60	0.44	<0.01	0.16	59	7.12
Long Prairie River at Philbrook, 313th Ave	mobilizing	0.71	0.11	0.02	0.02	279	0.10	0.04	0.02	274	-5.65
Lost River nr Brooks, CR119	chemodynamic	0.68	0.11	0.24	0.02	79	0.42	<0.01	0.15	67	273.75
Maple River nr Rapidan, CR35	mobilizing	0.37	0.56	<0.01	0.50	216	0.62	<0.01	0.49	205	11.2
Maple River nr Sterling Center, CR18	mobilizing	0.34	0.24	<0.01	0.22	269	0.33	<0.01	0.26	254	36.51
Middle Branch Root River nr Fillmore, CSAH5	mobilizing	0.72	0.53	<0.01	0.32	121	0.60	<0.01	0.33	113	12.67
Middle Fork Crow River nr Manannah, CSAH30	mobilizing	1.57	0.91	<0.01	0.28	70	0.83	<0.01	0.25	67	-8.82
Middle Fork Zumbro River nr Oronoco, 5th St	mobilizing	0.75	0.58	<0.01	0.50	127	0.62	<0.01	0.51	119	6.60
Middle River at Argyle, MN	mobilizing	0.49	0.16	<0.01	0.11	99	0.17	<0.01	0.10	96	3.79
Minnesota River at Judson, CSAH42	mobilizing	0.79	0.52	<0.01	0.21	433	0.53	<0.01	0.19	419	1.36



Minnesota River at Morton, MN	mobilizing	0.77	0.26	<0.01	0.06	299	0.28	<0.01	0.07	292	9.18
Minnesota River nr Lac qui Parle, MN	mobilizing	0.9	0.31	0.01	0.05	165	0.35	<0.01	0.06	162	12.09
Mississippi River at Grand Rapids, MN	mobilizing	1.32	0.27	<0.01	0.06	184	0.42	<0.01	0.11	171	56.08
Mississippi River nr Bemidji, CSAH11	chemodynamic	1.13	-0.22	0.18	0.04	44	-0.19	0.32	0.03	41	-16.08
Mississippi River nr Bemidji, MN	chemodynamic	1.89	-0.02	0.92	0.00	42	-0.12	0.66	0.01	38	449.62
Mud River nr Grygla, MN89	mobilizing	1.01	0.29	<0.01	0.17	157	0.40	<0.01	0.23	142	40.11
Mustinka River nr Norcross, MN9	mobilizing	0.58	0.41	<0.01	0.20	91	0.62	<0.01	0.30	85	51.09
Nemadji River nr Pleasant Valley, MN23	mobilizing	0.88	0.30	<0.01	0.31	68	0.28	<0.01	0.26	62	-7.72
North Fork Crow River nr Cokato, CSAH4	mobilizing	1.49	0.90	<0.01	0.19	74	1.02	<0.01	0.21	71	14.2
North Fork Crow River nr Rockford, Farmington Ave	mobilizing	1.05	0.33	<0.01	0.07	206	0.32	<0.01	0.06	202	-4.36
North Fork Whitewater River at Elba, Whitewater Dr	mobilizing	0.99	0.93	<0.01	0.68	82	0.94	<0.01	0.68	80	1.08
North Fork Zumbro River nr Mazeppa, CSAH7	mobilizing	0.90	0.58	<0.01	0.40	99	0.60	<0.01	0.39	95	2.88
Otter Tail River at Breckenridge, CSAH16	mobilizing	3.26	1.21	<0.01	0.22	231	1.35	<0.01	0.24	220	11.46
Otter Tail River nr Elizabeth, MN	chemodynamic	3.18	0.15	0.32	0.01	70	0.21	0.23	0.02	63	41.57
Pelican River nr Fergus Falls, MN210	mobilizing	1.27	0.49	0.01	0.09	77	0.60	<0.01	0.11	72	23.70
Pine River nr Jenkins, CSAH15	chemodynamic	0.62	0.23	0.21	0.08	22	0.36	0.10	0.15	20	60.81
Pipestone Creek nr Pipestone, CSAH13	mobilizing	0.55	0.60	<0.01	0.55	73	0.71	<0.01	0.56	66	18.10



Pomme De Terre River at Appleton, MN	mobilizing	1.07	0.95	<0.01	0.33	166	0.94	<0.01	0.33	164	-0.47
Pomme de Terre River nr Hoffman, CR76	mobilizing	1.94	0.91	<0.01	0.25	110	1.25	<0.01	0.32	103	38.26
Poplar River nr Lutsen, 0.2mi US of MN61	chemodynamic	0.75	0.05	0.20	0.01	167	0.04	0.42	0.00	160	-29.4
Prairie River nr Taconite, MN	chemodynamic	0.56	-0.13	0.08	0.05	59	-0.18	0.05	0.08	53	33.85
Rapid River at Clementson, MN11	mobilizing	0.51	0.04	0.05	0.01	309	0.01	0.66	0.00	296	-74.51
Red Lake River at Fisher, MN	mobilizing	0.81	0.71	<0.01	0.34	383	0.77	<0.01	0.35	366	7.81
Red Lake River at High Landing nr Goodridge, MN	mobilizing	4.74	0.65	0.01	0.11	59	0.90	<0.01	0.17	53	37.65
Red Lake River at Red Lake Falls, CR13	mobilizing	1.47	0.93	<0.01	0.42	121	1.00	<0.01	0.39	113	6.80
Red River of the North nr Kragnes, CSAH26	chemodynamic	0.32	-0.02	0.46	0.00	376	0.00	0.89	0.00	369	-80.69
Redwood River at Russell, CR15	mobilizing	0.61	0.28	<0.01	0.12	104	0.34	<0.01	0.13	97	21.16
Redwood River nr Redwood Falls, MN	diluting	0.66	-0.10	<0.01	0.02	327	-0.20	<0.01	0.10	316	96.5
Rock River at Luverne, CR4	mobilizing	0.64	0.71	<0.01	0.52	194	0.71	<0.01	0.51	190	0.10
Rum River at Anoka, headwater side of dam	mobilizing	0.72	0.37	<0.01	0.14	171	0.38	<0.01	0.14	170	1.48
S Br. Wild Rice River at CR27 nr Felton, MN	mobilizing	0.32	0.29	<0.01	0.29	48	0.30	<0.01	0.26	44	2.91
Sand Hill River at Climax, MN, US-75	mobilizing	0.41	0.50	<0.01	0.43	331	0.51	<0.01	0.43	322	2.12
Sandhill River nr Fertile, 450th St SW	mobilizing	0.70	0.47	<0.01	0.23	104	0.52	<0.01	0.23	94	9.61
Sauk River nr St. Martin, CR12	mobilizing	1.27	0.83	<0.01	0.30	60	1.01	<0.01	0.37	56	21.66
Second Creek nr Aurora, 0.6mi us of CSAH110	mobilizing	1.48	0.18	0.04	0.04	108	0.20	0.06	0.04	99	8.43



Seven Mile Creek nr St. Peter, 0.6mi us of US169	mobilizing	0.56	0.41	<0.01	0.39	326	0.40	<0.01	0.33	304	-2.53
Shakopee Creek nr Benson, 20th Ave SW	mobilizing	0.75	0.46	<0.01	0.13	135	0.76	<0.01	0.28	130	64.74
Shell Rock River nr Gordonsville, CSAH1	diluting	1.69	-0.73	<0.01	0.29	192	-0.73	<0.01	0.28	189	-0.47
Sleepy Eye Creek nr Cobden, CR8	mobilizing	0.51	0.42	<0.01	0.44	118	0.43	<0.01	0.40	110	3.6
Snake River above Warren, MN	mobilizing	0.44	0.22	<0.01	0.12	78	0.21	<0.01	0.11	77	-5.76
Snake River nr Big Woods, MN220	chemostatic	0.26	0.12	<0.01	0.13	327	0.12	<0.01	0.13	325	0.48
Snake River nr Pine City, MN	mobilizing	0.57	0.23	<0.01	0.11	213	0.22	<0.01	0.10	206	-4.32
South Branch Buffalo River nr Glyndon, 28th Ave S	chemostatic	0.28	0.20	<0.01	0.17	105	0.29	<0.01	0.24	98	49.53
South Branch Middle Fork Zumbro River nr Oronoco,5th St	mobilizing	0.59	0.49	<0.01	0.39	103	0.52	<0.01	0.40	100	6.68
South Branch Root River at Lanesboro, Rochelle Ave N	mobilizing	1.05	0.79	<0.01	0.47	127	0.80	<0.01	0.45	120	1.00
South Branch Two Rivers at Hallock, MN175	mobilizing	0.46	0.21	<0.01	0.11	104	0.28	<0.01	0.14	100	33.96
South Branch Two Rivers at Lake Bronson, MN	mobilizing	0.46	0.17	0.01	0.07	89	0.17	0.02	0.06	86	1.82
South Fork Crow River at Delano, Bridge Ave	mobilizing	0.53	0.10	0.05	0.02	212	0.12	0.03	0.02	206	16.77
South Fork Watonwan River nr Madelia, CSAH13	mobilizing	0.94	0.21	<0.01	0.08	123	0.31	<0.01	0.13	117	46.6
South Fork Zumbro River nr Oronoco, CR121	mobilizing	0.86	0.18	<0.01	0.06	126	0.23	<0.01	0.09	120	31.70



Split Rock Creek nr Jasper, 201st St	mobilizing	0.52	0.60	<0.01	0.50	171	0.59	<0.01	0.47	165	-2.05
Spring Creek nr Hanley Falls, 480th St	chemodynamic	0.49	-0.07	0.26	0.01	106	0.02	0.77	0.00	99	133.05
St. Francis River nr Big Lake, 164th St	chemodynamic	0.78	-0.17	0.27	0.02	61	-0.16	0.32	0.02	56	-2.19
St. Louis River at Floodwood, CSAH8	mobilizing	0.99	0.24	<0.01	0.09	87	0.30	<0.01	0.12	82	21.11
St. Louis River at Scanlon, MN	mobilizing	1.08	0.24	<0.01	0.11	138	0.20	<0.01	0.06	127	-16.9
St. Louis River nr Forbes, US53	mobilizing	0.58	0.15	0.01	0.06	120	0.13	0.05	0.03	111	-13.42
Stony River nr Babbitt, Tomahawk Rd	chemodynamic	0.9	0.04	0.70	0.00	76	-0.13	0.33	0.01	70	419.25
Straight River nr Faribault, MN	mobilizing	0.50	0.34	<0.01	0.28	111	0.35	<0.01	0.28	109	2.89
Sunrise River at Sunrise, CR88	chemodynamic	0.51	-0.04	0.53	0.00	90	-0.02	0.81	0.00	86	-57.9
Swan River nr Jacobson, CR438	chemodynamic	0.94	-0.19	0.20	0.03	55	-0.22	0.24	0.03	51	14.27
Swan River nr Sobieski, MN238	mobilizing	1.06	0.52	<0.01	0.26	62	0.57	<0.01	0.27	59	9.49
Tamarac River nr Florian, CSAH1	mobilizing	0.73	0.18	<0.01	0.14	111	0.26	<0.01	0.17	101	41.22
Tamarac River nr Stephen, CSAH22	mobilizing	0.38	0.25	<0.01	0.29	289	0.24	<0.01	0.27	287	-2.40
Thief River downstream of CSAH 7, 6 mi E of Holt	mobilizing	1.53	0.11	0.05	0.02	161	0.06	0.34	0.01	155	-45.73
Thief River nr Thief River Falls, MN	mobilizing	0.83	0.14	<0.01	0.05	421	0.13	<0.01	0.04	410	-1.92
Turtle Creek at Austin, 43rd St	mobilizing	0.92	0.58	<0.01	0.21	103	0.72	<0.01	0.24	94	23.05
Twelvemile Creek nr Wheaton, CSAH14	mobilizing	0.32	0.15	0.02	0.07	84	0.33	<0.01	0.20	79	117.23
Two Rivers nr Bowlus, 40th St	chemodynamic	0.88	-0.16	0.47	0.03	21	-0.16	0.47	0.03	21	0



Two Rivers nr Hallock, CSAH16	mobilizing	0.46	0.29	<0.01	0.35	303	0.27	<0.01	0.30	294	-5.38
Watonwan River nr Garden City, CSAH13	mobilizing	0.66	0.45	<0.01	0.38	360	0.42	<0.01	0.32	345	-6.66
Watonwan River nr La Salle, CSAH3	mobilizing	0.44	0.22	<0.01	0.12	140	0.30	<0.01	0.18	134	38
Wells Creek nr Frontenac, US61	mobilizing	1.57	1.26	<0.01	0.59	56	1.26	<0.01	0.58	54	-0.52
West Branch Lac qui Parle River at Dawson, Diagonal St	mobilizing	0.47	0.25	<0.01	0.12	64	0.42	<0.01	0.22	60	67.62
West Branch Rum River nr Princeton, CR102	chemodynamic	0.33	0.15	0.12	0.10	25	0.15	0.12	0.10	25	0
West Fork Des Moines River at Jackson, River St	chemodynamic	1.57	-0.04	0.59	0.00	165	-0.05	0.56	0.00	160	16.04
West Fork Des Moines River nr Avoca, CSAH6	mobilizing	0.69	0.60	<0.01	0.33	77	0.80	<0.01	0.41	72	34.59
Whitewater River nr Beaver, CSAH30	mobilizing	1.28	0.82	<0.01	0.53	206	0.83	<0.01	0.53	201	0.52
Wild Rice River at Hendrum, MN	mobilizing	0.48	0.43	<0.01	0.36	402	0.46	<0.01	0.36	388	7.08
Wild Rice River at Twin Valley, MN	mobilizing	0.75	0.58	<0.01	0.49	57	0.55	<0.01	0.39	53	-3.98
Wild Rice River nr Mahnommen, CSAH25	mobilizing	0.73	0.22	0.04	0.10	43	0.36	0.03	0.13	38	60.21
Yellow Bank River nr Odessa, CSAH40	mobilizing	0.52	0.55	<0.01	0.45	177	0.56	<0.01	0.44	173	1.26
Yellow Medicine River nr Granite Falls, MN	mobilizing	0.7	0.35	<0.01	0.25	257	0.34	<0.01	0.23	249	-2.22
Yellow Medicine River nr Hanley Falls, CR18	mobilizing	0.7	0.46	<0.01	0.34	119	0.48	<0.01	0.30	112	3.82
Zumbro River at Kellogg, US61	mobilizing	1.03	0.59	<0.01	0.38	229	0.60	<0.01	0.37	220	2.57



Table A6. Conditional Permutation Importance value for predictor variables used in the random forest model.

Predictor variable	Importance value
PctCrop2019CatRp100	0.009498
PctCrop2019WsRp100	0.009437
KffactCat	0.009059
PermCat	0.005716
AgKffactWs	0.005292
PctMxFst2019WsRp100	0.005098
PctUrbOp2019CatRp100	0.004543
Precip_Minus_EVTWs	0.004364
ClayWs	0.004223
PctWdWet2019WsRp100	0.004041
PctGrs2019Ws	0.003979
Pestic97Cat	0.00388
MAST_2013	0.003805
Phos_Crop_UptakeWs	0.003715
FertWs	0.003536
WWTPAllDensWs	0.003328
SiO2Cat	0.003151
PctHay2019Cat	0.003151
RdCrSlpWtdCat	0.003115
PctImp2013CatRp100	0.003096
Al2O3Cat	0.003007
PctGlacLakeFineWs	0.002988
PctCrop2019Ws	0.00293
CompStrgthCat	0.00286
NsurpCat	0.002853
K2OCat	0.002668
AgKffactCat	0.002657



NABD_NIDStorWs	0.002568
PctMxFst2019Ws	0.002464
ElevWs	0.002449
PctOw2019Cat	0.002403
PctDecid2019CatRp100	0.002028
OmCat	0.002027
PctCrop2019Cat	0.001864
WaterInputCat	0.001863
FertCat	0.001784
PctDecid2019Cat	0.001709
NO3_2008Ws	0.001689
Phos_FertCat	0.001659
MAST_2014	0.001589
Na2OCat	0.001586
WaterInputWs	0.001507
RockNWs	0.001481
Pestic97Ws	0.001459
PctUrbMd2019CatRp100	0.001402
MSST_2014	0.001387
MgOCat	0.001343
MWST_2013	0.001315
PctHbWet2019Cat	0.001298
Fe2O3Cat	0.00127
PctShrb2019Ws	0.001265
HydrICondCat	0.00122
RdDensWs	0.001211
Phos_ManureCat	0.00121
PctWdWet2019Ws	0.001191
RdCrsWs	0.001175



NPDES DensWs	0.001156
PctImp2008Ws	0.001152
PctHbWet2019CatRp100	0.001149
MSST_2013	0.001115
NANIWs	0.001108
Precip8110Ws	0.001107
MAST_2009	0.001104
SepticWs	0.000991
Tmean8110Cat	0.000952
RunoffCat	0.000932
PctHbWet2019Ws	0.000893
SandCat	0.000878
SuperfundDensWs	0.000855
PctGlacTilLoamCat	0.000825
PctImp2013Cat	0.000805
NCat	0.000726
BFIWs	0.000721
PctImp2006WsRp100	0.000699
ManureWs	0.000695
TRIDensWs	0.000673
PctAlluvCoastWs	0.000662
CaOCat	0.000651
SandWs	0.00065
PctImp2019Cat	0.000636
PctHbWet2019WsRp100	0.000595
PctColluvSedWs	0.000576
PctBl2019Cat	0.000569
NH4_2008Ws	0.000547
PctGrs2019Cat	0.000543



PctImp2016Ws	0.000522
PctUrbHi2019WsRp100	0.000522
PctImp2004CatRp100	0.000521
Tmax8110Ws	0.00052
PctOw2019Ws	0.000495
KffactWs	0.000492
RdDensCat	0.00045
PctImp2016WsRp100	0.000447
MSST_2009	0.000422
CBNFCat	0.000417
WtDepWs	0.000408
PctImp2008Cat	0.000407
Phos_Crop_UptakeCat	0.000385
WWTPMinorDensWs	0.000353
RockNCat	0.00035
PctImp2013Ws	0.000327
Tmean8110Ws	0.000292
NO3_2008Cat	0.00029
PctUrbOp2019WsRp100	0.000271
PctImp2008WsRp100	0.000255
SWs	0.000224
PctShrb2019CatRp100	0.000215
Tmax8110Cat	0.000193
Phos_ManureWs	0.000193
PctAg2006Slp10Cat	0.000163
Fe2O3Ws	0.000162
WsAreaSqKm	0.000155
PctUrbHi2019CatRp100	0.000138
PctUrbOp2019Cat	0.000138



NPDES DensWsRp100	0.000119
DamNrmStorWs	0.000118
SiO2Ws	0.000107
SuperfundDensWsRp100	9.66E-05
SCat	9.62E-05
CBNFWs	9.18E-05
PctAlluvCoastCat	9.11E-05
PctImp2001WsRp100	7.41E-05
PctGlacLakeCrsCat	6.86E-05
PctImp2001Ws	5.81E-05
PctWdWet2019CatRp100	4.87E-05
PctColluvSedCat	4.61E-05
PctHydricWs	4.17E-05
PctConif2019CatRp100	3.80E-05
PctGlacLakeCrsWs	1.37E-05
PctGlacTilClayCat	2.25E-07
DamNIDStorCat	0
SuperfundDensCat	0
TRIDensCat	0
MineDensCat	0
PctGlacTilCrsCat	0
PctHydricCat	0
PctGlacTilCrsWs	0
NABD_NrmStorCat	0
WWTPMajorDensCat	0
DamDensCat	-9.36E-07
ElevCat	-2.85E-06
RckDepCat	-9.76E-06
NABD_DensCat	-1.13E-05



DamNrmStorCat	-4.34E-05
PctWaterWs	-5.11E-05
NPDES DensCat	-6.43E-05
PctImp2011WsRp100	-7.86E-05
PctUrbLo2019Ws	-8.75E-05
ClayCat	-8.98E-05
PctHay2019WsRp100	-9.78E-05
CatAreaSqKm	-0.00011
NABD_NIDStorCat	-0.00011
PctUrbLo2019CatRp100	-0.00012
PctAg2006Slp20Ws	-0.00012
WWTPMajorDensWs	-0.00013
P2O5Cat	-0.00013
PctShrb2019WsRp100	-0.00014
PctOw2019WsRp100	-0.00016
RdCrSslpWtdWs	-0.00016
SepticCat	-0.00016
PctBl2019CatRp100	-0.00019
PctHay2019CatRp100	-0.00019
PctImp2006CatRp100	-0.00021
CompStrgthWs	-0.00022
PctUrbMd2019Ws	-0.00022
MgOWs	-0.00023
PctConif2019Ws	-0.00024
SN_2008Cat	-0.00024
PctAg2006Slp20Cat	-0.00026
PctUrbLo2019WsRp100	-0.00028
PctGlacLakeFineCat	-0.00028
RdDensCatRp100	-0.00029



PctImp2013WsRp100	-0.0003
TRIDensWsRp100	-0.00031
MineDensWs	-0.00032
PctImp2019CatRp100	-0.00037
CaOWs	-0.00037
WWTPMinorDensCat	-0.00037
Al2O3Ws	-0.00038
NANICat	-0.00039
PctImp2011Cat	-0.00039
PctUrbHi2019Ws	-0.00039
PctGrs2019WsRp100	-0.00039
PctShrb2019Cat	-0.0004
NH4_2008Cat	-0.00042
PctGlacTilClayWs	-0.00043
PctImp2001Cat	-0.00045
RckDepWs	-0.00046
HydrICondWs	-0.00048
Na2OWs	-0.00049
NABD_NrmStorWs	-0.00049
PctImp2004Ws	-0.00049
WWTPAllDensCat	-0.00054
PermWs	-0.00055
PctMxFst2019CatRp100	-0.00056
BFCat	-0.00056
PctImp2019WsRp100	-0.00058
NsurpWs	-0.00059
MineDensWsRp100	-0.00063
P2O5Ws	-0.00065
PctDecid2019WsRp100	-0.00067



PctImp2004Cat	-0.00069
PctImp2011Ws	-0.00077
PctConif2019Cat	-0.00077
PctImp2011CatRp100	-0.00078
NWs	-0.00081
PctGlacTilLoamWs	-0.00086
PctImp2008CatRp100	-0.00086
PctBl2019Ws	-0.00094
InorgNWetDep_2008Ws	-0.00098
Tile_density	-0.00099
PctMxFst2019Cat	-0.00099
PctImp2004WsRp100	-0.001
Tmin8110Ws	-0.001
MAST_2008	-0.00106
DamNIDStorWs	-0.00106
Phos_FertWs	-0.00107
PctConif2019WsRp100	-0.0011
PctImp2001CatRp100	-0.00112
RdDensWsRp100	-0.00113
PctUrbOp2019Ws	-0.00115
WtDepCat	-0.00116
Tmin8110Cat	-0.00119
RunoffWs	-0.00126
PctDecid2019Ws	-0.00138
PctWdWet2019Cat	-0.0014
PctImp2016CatRp100	-0.00142
SN_2008Ws	-0.00144
RdCrsCat	-0.00147
PctOw2019CatRp100	-0.00152



Precip8110Cat	-0.00156
PctImp2006Ws	-0.00159
ManureCat	-0.00159
PctUrbHi2019Cat	-0.00165
NABD_DensWs	-0.00166
PctImp2019Ws	-0.00169
PctUrbLo2019Cat	-0.00173
Precip_Minus_EVTcat	-0.0018
OmWs	-0.00182
PctAg2006Slp10Ws	-0.00183
K2OWs	-0.00184
PctUrbMd2019Cat	-0.00185
PctImp2006Cat	-0.00186
PctImp2016Cat	-0.00196
CanalDensWs	-0.00198
InorgNWetDep_2008Cat	-0.00209
PctUrbMd2019WsRp100	-0.00229
PctGrs2019CatRp100	-0.00232
DamDensWs	-0.00232
PctBl2019WsRp100	-0.00248
CanalDensCat	-0.00281
MSST_2008	-0.003
PctHay2019Ws	-0.00345